IOWA STATE UNIVERSITY
Digital Repository

1998

Combination of capillary isoelectric focusing and liquid chromatography with electrospray ionization mass spectrometry for protein characterization

Jing Wei

Iowa State University

INFORMATION TO USERS

Combination of capillary isoelectric focusing and liquid chromatography with

electrospray ionization mass spectrometry for protein characterization

by

Jing Wei

A dissertation submitted to the graduate faculty

in partial fulfillment of the requirements for the degree of

DOCTOR OF PHILOSOPHY

Major: Analytical Chemistry

Major Professor: Cheng S. Lee

Iowa State University

Ames, Iowa

1998

UMI Number: 9841097

UMI

300 North Zeeb Road
Ann Arbor, MI 48103

Graduate College
Iowa State University

This is to certify that the Doctoral Dissertation of

Jing Wei

has met the thesis requirement of Iowa State University

ʼ Major Professor

For the Major Program

For the Graduate College

TABLE OF CONTENTS

GENERAL INTRODUCTION

Dissertation Organization

This dissertation begins with a general introduction of the theory and the literature which provides background and recent progress in this area. Three research papers follow the general introduction with their literature cited. Finally, a general summary presents comments on this work and a list of cited references for the general introduction concludes this dissertation.

Capillary Electrophoresis

Electrophoresis has been one of the most widely used techniques for the separation and analysis of ionic substances. There is no doubt that gel electrophoresis has been an invaluable analytical tool for modern biochemical research; however, gel electrophoresis suffers from several disadvantages including the cumbersome and time consuming process of preparing the gels, the slow speed of separation, and poor reproducibility and resolving power. The use of a capillary as a migration channel presents a unique approach to separation and has advantages over the standard solid support approach. The physical characteristics of narrow bore capillaries makes them ideal for electrophoresis. With the a typical i. d. of 20 to 100 μm, the high surface-to-volume ratio of capillaries allows for very

efficient dissipation of Joule heat generated from high applied fields. Capillary electrophoresis (CE) offers other advantages when compared to traditional gel electrophoresis, such as rapid and highly efficient separations of analytes in very small sample volumes. Separations are based on the differences in effective mobilities of analytes in electrophoretic media inside the capillary. A basic instrument for CE separation includes a fused-silica separation capillary, two buffer reservoirs, a high-voltage power supply, and a detector. Different separation modes of CE, such as capillary zone electrophoresis (CZE)[1,2], capillary gel electrophoresis (CGE)[3-5], capillary isotachophoresis (CITP)[6-8], capillary electrochromatography (CEC)[9], capillary isoelectric focusing (CIEF)[10-14],and micellar electrokinetic chromatography (MEKC)[15], can be performed using a standard CE instrument.

CZE is the most commonly used mode for the separation of ionic compounds in CE. The ionization of surface silanol groups in the fused-silica capillary at pH > 2 results in a negatively charged silica surface and an electrostatic diffuse layer of cations adjacent to the capillary wall. The migration of cations in the diffuse layer induces the electroosmotic flow toward the cathode. Ionic compounds with various charge to mass ratios exhibit different electrophoretic mobilities and are thus separated in CZE. Analytes with different sizes migrate through the pores of the gel matrix at different velocities and can be separated in CGE[3,4]. Because of the anti-convective media and the minimized solute diffusion, CGE has achieved the highest separation efficiency ever obtained by any analytical separation

technique to date. CITP is performed in a discontinuous buffer system[7,8]. Sample

components stack between the leading and terminating zones, and produce a steady-state

migrating configuration of consecutive sample zones. In CEC[9], the capillary is packed with

the material which can retain solutes by the partitioning phenomenon similar to that in

HPLC. The mobile phase in CEC is driven by electroosmotic flow and provides a higher

efficiency than the pressure-driven system of HPLC. In MEKC[15], surfactants are added to

the electrophoresis buffer at the concentration above the critical micelle concentration to form

micelles in equilibrium with the surfactant monomers. Differential partitioning of solutes

between the aqueous and the micellar phases in MEKC results in the separation of neutral

and ionic compounds.

CIEF was first described by Hjerten and Zhu in 1985[14] for the separation of

proteins based on their differences in isoelectric point (pI). In CIEF, the fused-silica capillary

is usually coated with linear polyacrylamide to eliminate the electroosmotic flow and protein

adsorption onto the capillary wall. The CIEF capillary is initially filled with a solution

containing the protein analytes and a mixture of carrier ampholytes. These ampholytes are

small amphoteric molecules containing both amino and carboxylic groups with different pIs.

Under the influence of applied electric field, the negatively charged acidic ampholytes migrate

toward the anode and decrease the pH at the anodic section, while the positively charged

ampholytes migrate toward the cathode and increase the pH at the cathodic section. These

pH changes continue until each ampholyte molecule reaches its pI. Because each ampholyte

molecule has its own buffering capacity, a continuous pH gradient is formed in the capillary. Figure 1 shows the mechanism of CIEF at the focusing step.

Protein analyte acquires a net negative charge in the region between its pI and cathodic end (where pH > pI) and migrates toward the anode. In contrast, protein analyte exhibits a net positive charge in the region between its pI and anodic end (where pH < pI) and migrates toward the cathode. As a result, protein molecules distributing over the entire capillary at the beginning of the experiment are focused at the regions where pH = pI. To prevent the ampholytes and analytes from migrating into the inlet (anode) and outlet (cathode) reservoirs by diffusion, solutions of 20 mM phosphoric acid and 20 mM sodium hydroxide are typically used as the anolyte and the catholyte, respectively.

Due to the focusing effect, CIEF thus permits analysis of very dilute protein samples with a typical concentration factor of 50-100 times. Furthermore, the analyte molecules leaving the focused zones by diffusion or convection migrate back to their pIs due to the same focusing effect. This zone-sharpening effect makes isoelectric focusing a high resolution tool for the analysis of proteins with a pI difference as small as 0.02 pH units[13].

In CIEF, the focused analyte zones must be mobilized and detected at one end of the capillary. The mobilization of CIEF is illustrated in Figure 2. Among various mobilization approaches, the hydrodynamic mobilization described by Hjerten and Zhu[3] involves the connection of a pump to the cathodic end of the capillary via a T-tube. The electric field is maintained during the mobilization step to help minimizing the hydrodynamic band

Separation Principle of CIEF

Focusing

Anode

Cathode

H_3PO_4

20 mM

NaOH

20 mM

pH Gradient: 3   pI   10

5
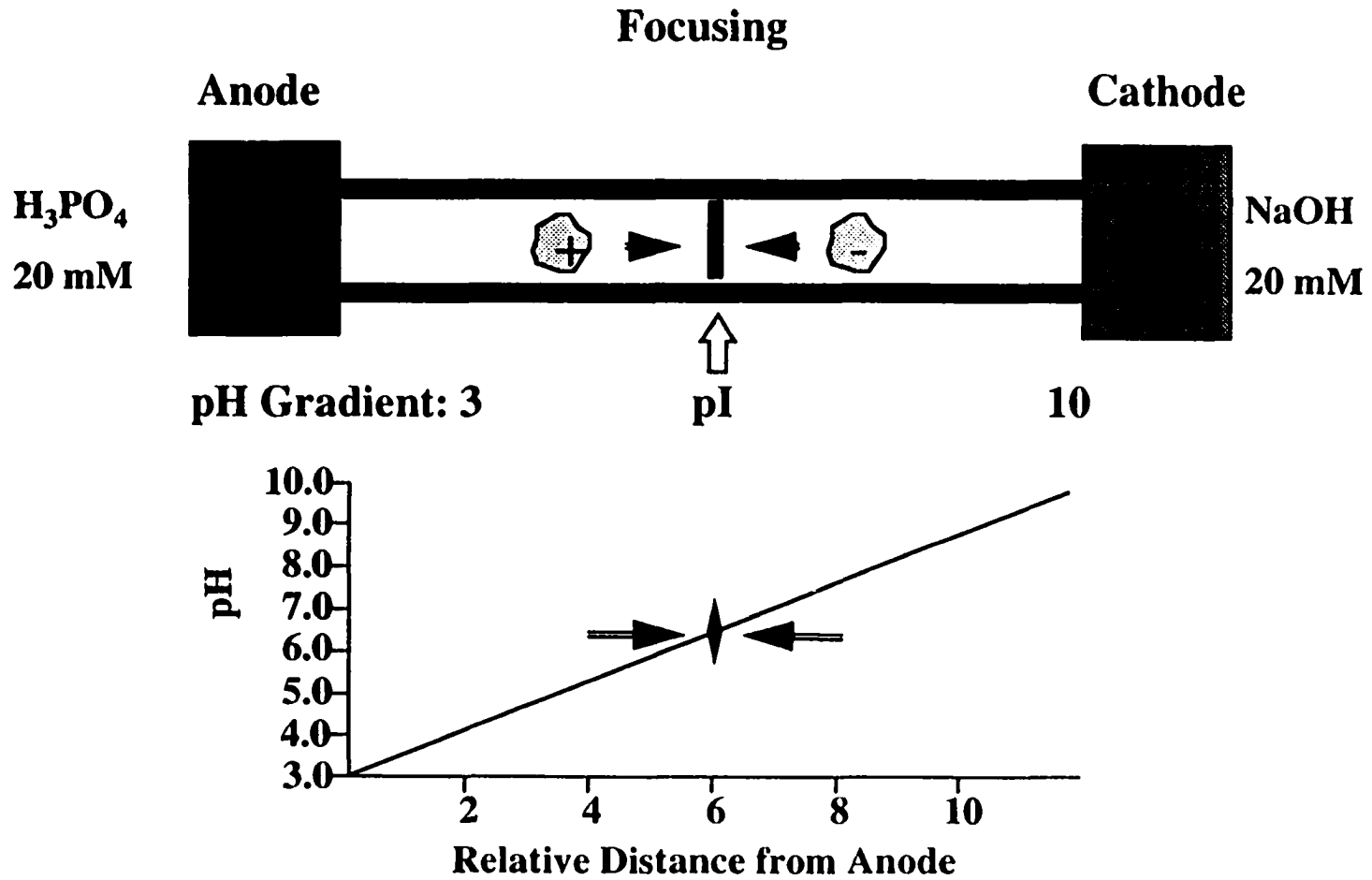
Figure 1. Focusing step of CIEF

Separation Principle of CIEF

Mobilization

A. Cathodic Mobilization

Anode

Cathode

H_3PO_4

20 mM

$H^+ \longrightarrow$

pH 3

$\longleftarrow OH^-$

$\longleftarrow OAc^-$

pH ↓

1% HOAc 50%

MeOH 49%

H_2O
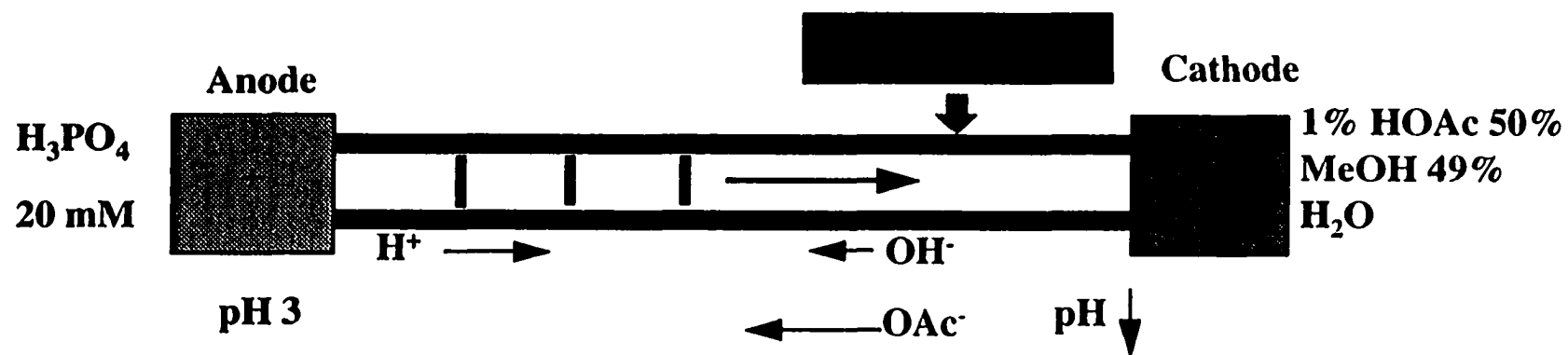
B. Gravity Mobilization

C. Pressure Mobilization

Figure 2. Mobilization step of CIEF

broadening. The so called salt mobilization[11,12] involves the replacement of the anolyte, 20 mM phosphoric acid, with 20 mM sodium hydroxide after the focusing is complete. This replacement under the influence of an electric field results in an increase of solution pH inside the CIEF capillary. The focused ampholytes and protein analytes are no longer neutral and become negatively charged with electrophoretic migration toward the anodic end of the capillary. This is referred to as anodic mobilization. On the contrary, the cathodic mobilization can be achieved by replacing the catholyte, 20 mM sodium hydroxide, with a 20 mM phosphoric acid solution after the focusing is complete.

Alternatively, a small amount of buffer additive such as 0.1% methyl cellulose can be added into the sample solution to suppress the electroosmotic flow in the uncoated capillary[10]. The electroosmotic flow is reduced sufficiently to ensure the complete focusing before the analytes migrate past the detection window. The analytes are focused and eluted by electroosmotic flow in one step. Since a bare silica capillary can be employed, the coating procedure is eliminated and the potential for instability of a coating is avoided.

Liquid Chromatography

The first commercial HPLC instrument was introduced in 1969. Since then, HPLC has progressed from a difficult "art" into one of the most important separation techniques used to solve a host of problems in the modern laboratory[16,17]. For a typicalHPLC system, The solvent reservoir is employed to store the mobile phase. The pump delivers the

mobile phase and is one of the most important components of HPLC since its performance directly affects retention time reproducibility and detector sensitivity. Analytes are introduced through the injector. The separation takes place in the column based on analytes' differential distribution between two phases: the stationary phase packed inside the column and the mobile phase delivered by the pump. As the sample components elute from the column, a suitable detector is used to monitor and transmit the signal to a recording device. The "chromatogram" is a record of the detector response as a function of time and indicates the presence of the analytes as "peaks". There are different forms of liquid chromatography including normal-phase, reversed-phase, size exclusion, ion exchange, and bioaffinity.

In normal-phase chromatography[18,19], the retention is governed by the interaction of the polar parts of the stationary phase and solute. For the retention to occur in normal-phase, the stationary phase must be more polar than the mobile phase. Normal-phase chromatography separates compounds that differ in the number or chemical nature of their polar groups with the nonpolar components emerging from the column first. Size exclusion chromatography is a simple molecule size classification process rather than any interaction phenomena forms the basis of separation. The smaller molecules migrate into more of the smaller pores of the cross-linked polymer gel than the larger molecules in the sample. Analyte molecules that are too large to diffuse into any pores are excluded at V_i (interparticle volume) while the molecules that are small enough to penetrate all the pores are eluted at the breakthrough volume, V_o. All other components elute between V_i and V_o with the larger molecules eluting first. In ion exchange chromatography, the stationary phase is characterized

by the presence of charged centers bearing exchangeable counterions. Retention is based on the attraction between solute ions and charged sites bound to the stationary phase. The fundamental principle of bioaffinity chromatography consists of the utilization of biologically active substances to form stable, specific, and reversible complexes[20]. The formation of the biologically functioning complexes involves the participation of common molecular forces such as van der Waal's interaction, electrostatic interaction, dipole-dipole interaction, hydrophobic interaction, and hydrogen bonding.

Reversed-phase chromatography[16,17] (RP-LC) is characterized by a polar mobile phase in conjunction with a nonpolar stationary phase. The most commonly used stationary phase for reversed-phase chromatography is an octadecyl alkyl hydrocarbon chain (C_{18}) which is chemically bonded to the silica substrate. Typical mobile phases are mixtures of methanol/water and acetonitrile/water. Reversed-phase chromatography can be used to separate a broad spectrum of non-ionic, ionizable, and ionic compounds. Retention in reversed-phase chromatography occurs by non-specific hydrophobic interactions of the solutes with the stationary phase. The near universal application of reversed-phase chromatography stems from the fact that virtually all organic molecules have hydrophobic regions in their structures and are capable of interacting with the stationary phase.

The mobile phase of RP-LC is made by choosing one solvent in which the sample is very soluble and another solvent in which the sample is less soluble. One can then prepare a mobile phase by adjusting the amounts of the "strong" and "weak" solvents to a ratio where the attraction of the solutes to stationary phase is in a competitive equilibrium with the

attraction (solubility) of the solutes to the mobile phase. The equilibrium of the solutes in the mobile phase relative to that in the stationary phase determines the retention time and effects the separation. The selectivity of reversed-phase chromatography may be conveniently adjusted by changing the type of organic modifier in the mobile phase. For ionic or ionizable solutes, pH buffers which suppress ionization, or ion-pairing reagents used to form lipophilic complexes, increase the degree of solute transfer to the stationary phase and may be used to control selectivity.

According to the solvophobic theory[20,21], hydrophobic interactions result from repulsive forces between a polar solvent and the nonpolar solute and stationary phase. The solvophobic theory assumes that aqueous mobile phases are highly structured due to the tendency of water molecules to self-associate by hydrogen bonding. As a consequence of the very high cohesive energy of the solvent, the less polar solutes are literally "squeezed out" of the mobile phase and are bound to the hydrocarbon portion of the stationary phase. The driving force in the binding of the solute to the stationary phase is the decrease in the area of the nonpolar segment of the solute molecule exposed to the solvent.

Hydrophobic selectivity in reversed-phase chromatography arises as a consequence of differences in the nonpolar surface areas of different solutes. Reversed-phase chromatography is thus the preferred technique for separating homologous samples. Within a homologous series, the logarithm of the capacity factor is generally a linear function of the carbon number[22]. Branched chain compounds are generally retained to a lesser extent than their straight chain analogs and unsaturated compounds are eluted before the corresponding

saturated analogs. Reversed-phase chromatography is also gaining increasing attention as a method for separating biological molecules such as proteins and peptides because the hydrocarbon-like stationary phases equilibrate rapidly with changes in mobile phase composition and are therefore suitable for use with gradient elution[23,24].

Mass Spectrometry

Electrospray Ionization

In the last few years, electrospray ionization mass spectrometry (ESI MS) has revolutionized the study of large biomolecules. Dole et. al.[25] took the first step as the forerunner of modern ESI techniques in studding the pneumatically generated ion by gas phase mobility. In the early 1980s, Fenn and coworkers[26-28] further developed fundamental aspect of the technique and introduced an electrospray source coupled to a quadrupole analyzer. The ease of use and accuracy of this technique for molecular weight determination has led to an acceleration of research in the field of proteins and nucleic acids using mss spectrometry.

An electrospray[29-31] is produced by applying a strong electric field, under atmospheric pressure, to a liquid passing through a capillary tube with a week flux (normally 1-10 μl/min). Under the influence of a positive electric field applied at capillary terminus, the positive ions accumulate on the solution surface, which will break to form highly charged

droplets. The solvent contained by the droplet evaporates, which causes them to shrink to the point where the repelling coulombic forces come close to their cohesion forces, thereby causing their explosion. These droplets undergo a cascade of ruptures, yielding smaller and smaller droplets until the elecrtic field on their surface becomes large enough to produce the desorption of the ions[32]. The ions that are thus obtained carry a great number of charges if several ionizable sites are present on the molecule. The ions formed at atmospheric pressure are then channeled into the high vacuum of the mass spectrometer through a capillary or a set of differentially pumped skimmers.

The ESI mass spectra normally correspond to a statistical distribution of consecutive peaks characteristic of multiply charged molecular ions obtained through protonation $(M+zH)^{z^{.}}$, while avoiding the contributions from dissociations or from fragmentations. Obtaining multiply charged ions is advantageous as it improves the sensitivity and it allows the analysis of high molecular weight molecules using analyzers with a weak nominal mass limit. Indeed, the technical characteristics of mass spectrometers are such that the value being measured is not the mass, but rather the mass to charge ratio.

A variety of algorithms have been developed to allow the determination of the molecular mass through the transformation of the multiply charged peaks present in the ESI spectrum into singly charged peaks. Some also allow the deconvolution of a mixture ESI spectra; However, the complexity of the spectra obtained for an isolated compound is such that only simple mixtures can be analyzed.

Several features of ESI have contributed to its great success and significance in various biological and biomedical applications. First, ESI can be employed for the direct interfacing of MS with HPLC or CE separations. Furthermore, the multiple charging phenomenon in ESI allows the determination of molecular weight of macromolecules over 50 kDa using a mass spectrometer with limited m/z range. When averaged, these multiple-charged ions provide excellent accuracy and precision in the mass determination of macromolecules[33-35]. Finally, ESI is probably the 'softest' of all ionization techniques yet developed, involving only the combination of high electric fields, moderated by an atmospheric pressure bath gas with typically only mild heating to enhance desolvation. Thus, the preservation of non-covalent association is possible in ESI. In fact, the application of ESI permits the measurements of non-covalent interactions between biological macromolecules, such as the heme-protein complex[36], enzyme-inhibitor complex[37], oligonucleotide duplex[38], and receptor-ligand complex[39-41].

Matrix Assisted Laser Desorption Ionization

Matrix assisted laser desorption/ionization(MALDI) was introduced in 1988 as a method of transferring and ionizing the intact, large, labile biopolymers into the gas phase[42]. Briefly, the technique involves mixing the analyte of interest with a large molar excess of a matrix compound, usually a weak organic acid, which strongly absorbs laser light. When an incident laser pulse strikes the solid matrix/analyte mixture, ablation and ionization

of the surface layer occur very rapidly. Remarkably, the fragile biomolecules remain intact and appear as molecular ions measured by time-of-flight mass spectrometry(TOF MS)[42-44]. The incorporation of matrix materials with analyte molecules overcomes molecular fragmentation during laser desorption/ionization by several means: (i) the matrix strongly absorbs the laser light at a wavelength at which the analytes are only weakly absorbing; (ii) the matrix reduces intermolecular contact beyond analyte-matrix interactions thereby reducing the energy necessary to desorb the molecules; (iii) the matrix acts as a protonating (positive ion detection) or deprotonating (negative ion detection) agent either in solution/solid phase or in gas phase and is therefore essential in the ion formation process. All these matrix effects are necessary and combine to provide high ion yields[45] of intact biopolymers, giving rise to sub-picomole sensitivity. Common matrices are benzoic acid and cinnamic acid derivatives for peptides and proteins, and picolinic acid and acetophenone derivatives for oligonucleotides.

Several theories including thermal spike model[46] and the pressure pulse theory[47] have been developed to explain the desorption of large molecules by MALDI. It is generally thought that the ionization is essentially chemical in nature, like a proton transfer or cationization reaction. The charge depends critically on the matrix-analyte combination but not on the number of acidic or basic groups of the macromolecule[48]. This suggests that a more complex interaction of analyte and matrix, rather than simple acid-base chemistry, is responsible for ionization.

Time of Flight Analyzers

Time-of-flight (TOF) analyzers were described by Wiley and Mclaren in 1955[49] and review papers were published by Cotter in 1992[44] and Wollnik in 1993[50]. The mass to charge ratio (m/z) of an ion can be measured by determining its velocity after acceleration in an electrical field. In practice, this is done by accelerating an ion electrostatically to a defined kinetic energy and measuring its time of flight through a field free region. The pulsed laser used for MALDI makes it an ideal technique for coupling with TOF MS since there is a precisely defined time of ion generation. A detector positioned at the end of the field free region determines the flight time for each ions. Typical features of TOF MS include:(i) a spectrum over the complete mass range can be obtained in microseconds;(ii) in principle, no upper mass limit exists for this type of mass analyzer; (iii) a very high sensitivity is achievable due to the high ion transmission; (iv) the operation is rather simple and straightforward.

A major limitation of MALDI-TOF MS has often been relatively poor mass resolution. Earlier studies by Beavis and Chait[51] and by Zhou et al.[52] indicated that the ions produced by MALDI exhibited a rather broad energy distribution. Initial velocity of desorbed analyte ions was nearly independent of mass; thus the initial kinetic energy was not proportional to mass of the analyte. In addition, when desorption occurred in a strong electrical field, energy was lost presumably by collisions with the neutral plume, and further mass dependent energy dispersion resulted.

Wiley and McLaren[49] described a technique which they named "time-lag energy focusing" for the correction of initial velocity distributions. The ions are produced in a field-free region, and the accelerating field was turned on by application of a fast pulse at a predetermined delay time after initial ion formation. Recently, Brown and Lennon[53], Colby et al.[54], and Whittal and Li[55] have applied similar focusing techniques to MALDI, and have shown significantly improved resolution for selected masses as a function of delay time and pulsed field intensity in the ion source.

In delayed ion extraction, a short time delay is inserted between the laser ionization and ion extraction events. The region inside the extraction grids is field-free during the delay. Following the delay, a pulsed potential is applied to extract the focused ions. Application of the appropriate pulsed voltage provides the energy correction necessary to simultaneously detect all ions of the same m/z regardless of their initial energy. A 200 ns time delay is typically used between desorption and ionization. The pulsed extraction potential is mass dependent; higher pulsed potentials is required for ions of higher mass.

The coupling of an electrospray source with a TOF mass spectrometer is difficult, since electrospray yields a continuous ion beam, whereas the TOF system works on a pulsed process. Ions from the electrospray (ESI) are carried to an ion trapping device by low-potential lenses and are stored there by a decelerating field. They are then extracted from the storage device and pass into the flight tube, which is perpendicular to the incident beam direction. This occurs through 1 µs pulses that can be repeated at a frequency as high as

1kHz. The perpendicular orientation of the source with respect to the flight tube reduces the

dispersion in kinetic energy in the direction of the flight tube. This gives a mass resolution of

25 000 in the case of high masses[56].

Quadrupolar Analyzers

The quadrupole is a device which uses the stability of the trajectories to separate ions

according to their m/z ratio.

Quadrupole analyzers are made up of four rods with circular or, ideally, hyperbolic

section. The filtering action of the quadrupole mass analyzer is obtained by the application

of combination of the time independent (dc) and a time dependent (ac) potential. The

stability of the ion motion within the quadrupole can be described using an a-q stability with

the definitions of a and q given by

$$a = 4eU/\omega^2 r_0^2 m \qquad (1)$$

$$q = 2eV/\omega^2 r_0^2 m \qquad (2)$$

U is the magnitude of the applied dc potential, V is the magnitude of the applied ac or rf

potential, ω is the angular frequency ($2\pi f$) of the applied ac waveform, r_0 is the distance from

the center axis (the z axis) to the surface of any electrode, m is the mass of the ion. The

stability diagram allows the operation of the quadrupole mass analyzer to be reduced from a

six-dimensional issue (involving e, ω, r_0, m, U, and V) to a two-dimensional problem involving

only the reduced parameters a and q. This results in a tremendous conceptual simplification that allows one to visualize readily the effects of various physical parameters on the operation of the quadrupole mass analyzer.

Quadrupole mass analyzers are now widely used in many areas of chemical analysis. For applications where extremely high resolution data or exact mass measurements are not required, quadrupoles offer a number of significant advantages over more traditional mass analyzers[57,58].

First, the short distance between the ion source and detector combined with the strong focusing properties of such devices make the quadrupole mass analyzer useful at comparatively high pressures ($\sim 10^{-5}$ torr). Second, quadrupoles resolve ions on the basis of their mass-to-charge ratios. Finally, a quadrupole mass analyzer is a mechanically simple instrument compared to other types of mass analyzers. Quadrupole devices do not rely on the use of magnetic fields for their mass discrimination. Thus, the slow scan speeds commonly associated with magnets are avoided.

The quadrupole is a real mass to charge analyzer. It does not depend on the kinetic energy of ions when they leave the source. The only requirement are, first, that the time for crossing the analyzer is short compared with the time necessary to switch from one mass to the other, and second, that the ions remain long enough between the rods for a few oscillations of the alternative potential to occur. This means that the kinetic energy at the source exit must range from one to a few hundred electron volts. These weak potentials in

the source allow a relatively large tolerance on the pressure. As the scanning velocity can be easily increased, this analyzer is well suite to CE or LC coupling.

Figure 3 shows the general diagram of an instrument with three quadrupoles. A collision gas, typically N_2, can be introduced into the central quadrupole at a pressure such that an ion entering the quadrupole undergoes several collisions. When the ion is inert, kinetic energy is transferred to the ion by converting a fraction of the collision energy into internal energy. The ion then fragments and the products are analyzed by the quadrupole Q3.

Capillary Electrophoresis- Mass Spectrometry Coupling

CE is a high efficiency separation method, while ESIMS allows the formation of multiple-charged ions directly from the electrophoresis eluent and the precise mass determination of high molecular weight ions. The combination of CE with ESIMS is very attractive for obtaining higher selectivity and for structural analysis of analytes in a MS/MS mode.

Capillary Electrophoresis-Electrospray Ionization Mass Spectrometry Interface

ESI incorporates analyte introduction into mass spectrometer by means of a flowing liquid and produces the gas phase ions directly from the CE running buffer and transports the gas ions from the atmospheric pressure region into the mass spectrometer as efficiently as
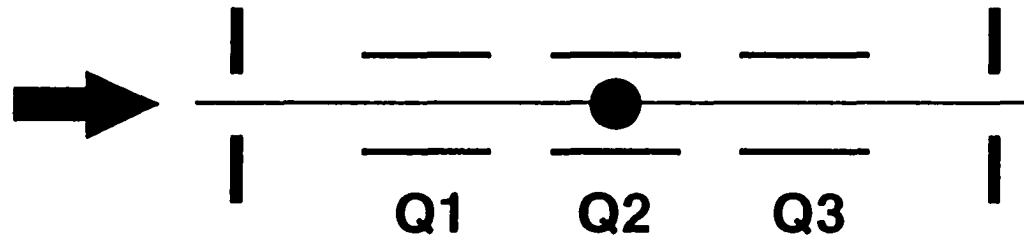
Figure 3. Diagram of a triplee quadrupoleoinstrumenent.
The First an the last (Q1 and Q3)are mass spectrometers.
The center quadrupole (Q2) is a collision cell made up
of a qudrupole using radiofrequency only.

possible. The first CE-ESIMS interface was described by Smith and his co-workers[59]. A stainless steel needle was employed to ensure electrical contact with the solution eluting out of the CE capillary, hence terminating the CE circuit and initializing the electrospray process. A less satisfactory method for making the electric contact between the electrophoretic buffer and the electrospray interface was made by depositing a thin metal film on the outer surface of the capillary instead of using a stainless steel needle[60].

Smith and his co-workers[61] also introduced an improved ESIMS interface equipped with a coaxial sheath liquid as shown in Figure 4. In this design, a fused-silica capillary protruded about 0.5 mm from a stainless steel needle. The sheath liquid usually consisted of a mixture of water and volatile organic solvent such as methanol. When the CE buffer was mixed with the sheath liquid at the end of the capillary, the surface tension decreased while the volatility increased, which enhanced the electrospray efficiency. Furthermore, the sheath liquid established electrical contact at the end of the capillary. The sheath potential was controlled around 5 kV (for positive ion mode) and functioned as both the CE cathodic potential and the electrospray voltage. A counter current flow of warm nitrogen gas (up to 80 °C) between the nozzle and the ESI source was used to aid desolvation, although sufficient heating during transport into the mass spectrometer also accomplished effective desolvation.

Lee et al.[62] developed a liquid junction coupling for CZE-ion spray MS (which is the nebulizing gas assisted ESIMS). The liquid junction and coaxial interfaces were compared by Pleasance et al.[63] and the coaxial sheath flow appeared to have several advantages with regard to ruggedness, ease of use, better sensitivity and electrophoretic performance. Gale

Schematic of On-line CIEF-ESIMS

CE System

Finnigan TSQ 700

Electrospray
Chamber

RF Only Octapole

Skimmer

Sheath
Liquid

Lens

Separation
Capillary

S.S. Needle

to mass
analyzer

H₃PO₄ 20mM

+15kv

+5kv

Heated
Capillary

1.1 TORR

10⁻⁶TORR

Current Sinking
Resistor (1GΩ)

Pump

Sheath
Liquid

Capillary

Electrospray

S.S.
Needle

Buffer/Sheath Conc

~1mm
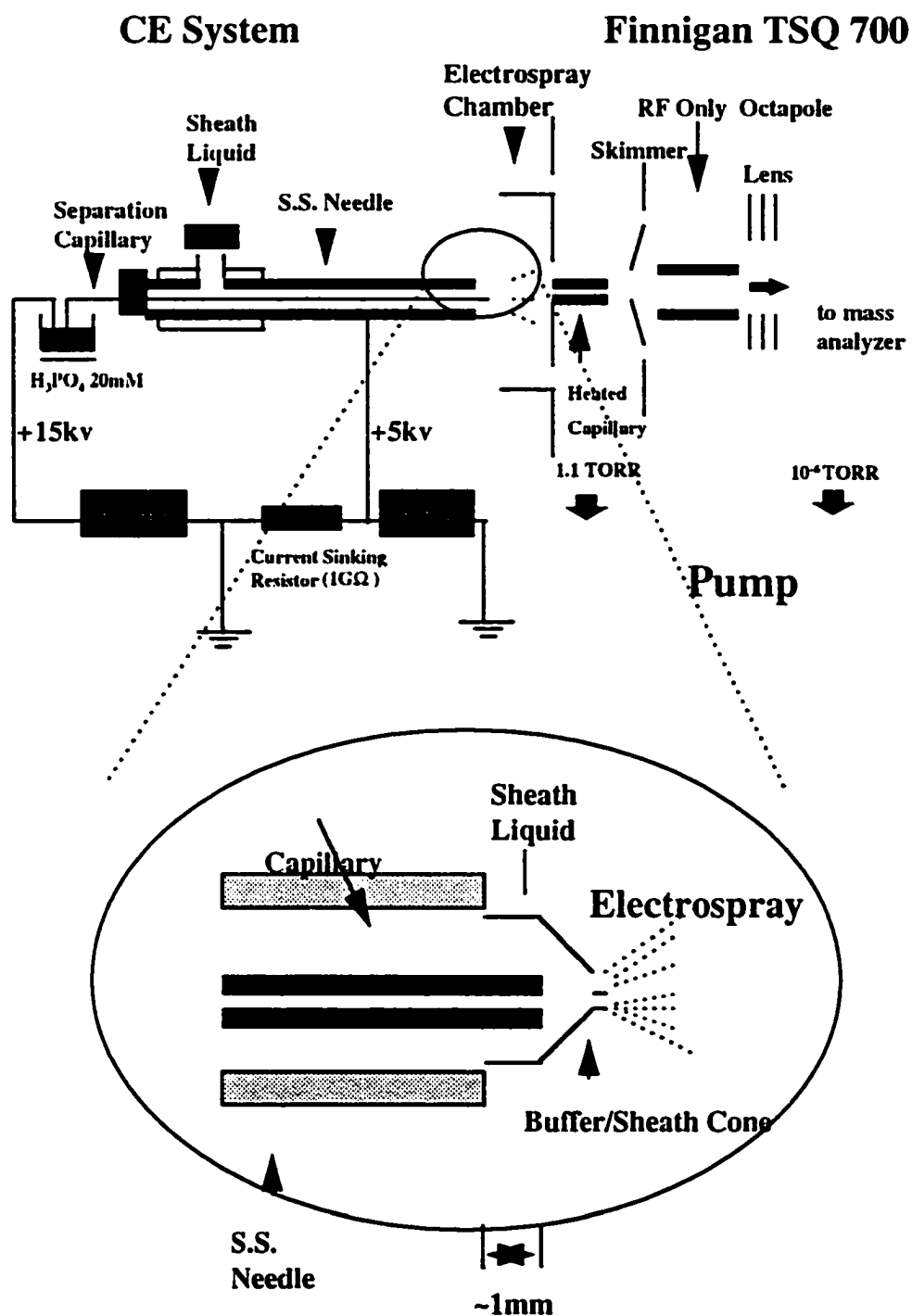
Figure 4. On-line CIEF-ESIMS set up

and Smith[64] described a sheathless ESI source in which a small diameter etched-tip capillary was incorporated. The ability to electrospray aqueous solutions without the use of an ancillary sheath flow was demonstrated with several biopolymers. Tsuji and his co-workers[65] introduced a simple procedure for preparing gold-coated silica capillaries used in ESIMS. The performance characteristics of these durable capillaries as continuous infusion sources were examined, and their utility in on-line CE-ESIMS was demonstrated.

Applications of Capillary Electrophoresis-Electrospray Ionization Mass Spectrometry for Proteins and Peptides

The multiple charging phenomenon in ESI makes the detection of biomacromolecules possible using a quadrupole mass spectrometer with limited m/z range. Various applications have been reported for the analysis of peptides and proteins by CE-ESIMS[66-69]. A reduced elution speed method[68] was described for the enhancement of detection sensitivity in CZE-ESIMS. Mass spectra for a set of standard proteins were obtained from 60 femtomole of proteins, while detection limits were down to the 24 fmol level for peptides[70]. The use of small i.d. capillaries for the detection of protein analytes at the attomole level was demonstrated by Smith and his co-workers[38]. With the proper selection of running buffers and on-line combination of transient CITP with ESIMS, the concentration

detection limits for a full scan were improved by a factor of 100 times, in comparison with CZE-ESIMS[69].

The application of CE/MS to peptide mapping, offering the potential for high separation efficiency combined with high information content, should be very desirable and widely used.

Chromatography - Mass Spectrometry Coupling

In order to analyze a mixture, a gas or liquid chromatographic (GC-MS or LC-MS) analyzer precedes the mass spectrometer. For LC-MS, the chromatographic products must be introduced one after the other into the spectrometer as a liquid from which ions can be extracted by electrospray, FAB, APCI or other ionization techniques.

The on-line combination of liquid chromatography and mass spectrometry (LC-MS) has been under investigation for over 20 years. The major difficulty in combining the two powerful analytical techniques is the apparent flow rate incompatibility as expressed in the need to introduce 1 ml/min of a liquid effluent from a conventional LC column into the high vacuum of the mass spectrometer.

Liquid chromatography-Mass Spectrometry Interface

Many efforts have been made in designing different LC-MS interfaces to solve the flow-rate incompatibility problem. Over the past 20 years, a total of about 25 different LC-MS interfaces have been described in the literature[71,72]. The ones that have demonstrated practical potential for real applications include moving-belt interface[73], thermospray interface[74], continuous-flow or dynamic fast-atom bombardment interface (CF-FAB)[75], particle-beam interface[76], atmospheric-pressure chemical ionization (APCI) interface[77], and electrospray ionization interface (ESI)[78,79].

In an ESI, the column effluent is nebulized into the atmospheric-pressure region as a result of the influence of a high electric field applied at the electrospray capillary tip. The solvent emerging from the capillary tip breaks into highly charged droplets, typically only a few micrometers in diameter. The charged droplets drift in the electric field between the capillary and the mass spectrometer sampling aperture. In transit through the MS interface, the droplets experience conditions that cause evaporation and droplet disintegration, leading ultimately to very small, highly charged droplets capable of producing gas-phase ions, either by ion emission or complete solvent evaporation. In some designs, the electrospray nebulization is assisted by pneumatic nebulization. Such an approach is called an ionspray interface[80].

Applications of Reversed-Phase LC-Electrospray Ionization Mass Spectrometry for Proteins

and Peptides

It is estimated that somewhere between 75-90% of all HPLC separations are carried

out in the reversed-phase mode[17] while electrospray ionization (ESI) has become one of the

leading sample introduction/ionization technique for MS[81]. Reversed-phase liquid

chromatography (RPLC)-electrospray ionization mass spectrometry (ESIMS) combines the

two most popular and powerful techniques together and has had a major impact in many

fields especially the bio-related areas of pure and applied science and technique.

RPLC-ESIMS is a well-established method for the identification and characterization

of proteins and peptides because of its inherent selectivity, specificity, and sensitivity. This

method is particularly valuable for analysis of mixtures because of the combined strengths of

LC to purify, concentrate, and resolve complex mixtures, and ESIMS for mass separation and

determination. Typical protocols for protein identification or characterization of

modifications begin with the enzymatic digestion of the protein sample, resulting in a

complex mixture of peptides. The separation of these mixtures by RPLC facilitates the task

of the interpretation of spectra in ESIMS.

Mass spectrometric methods have been developed for phosphopeptide-specific

detection in ESI MS or LC-ESI MS. The characteristic fragmentation processes[82] or

fragment-ion production[83] under collision-induced dissociation (CID) conditions were

exploited for the location of phosphorylation sites of phosphoprotein. The most specific

method by Covey et al. involves monitoring the characteristic neutral loss of phosphoric acid by phosphopeptides under CID and has been applied successfully to the determination of phosphorylation sites in casein by the direct infusion MS/MS in neutral loss mode[82]. Signals from unphosphopeptides are virtually eliminated, resulting in a spectrum with phosphopeptide ions. An alternative and complementary approach by Huddleston et al., termed LC/CID-MS, localized phosphopeptides in mixtures by the generation and detection of phosphate-specific fragment ions during LC/ESI-MS.

HIGH RESOLUTION ANALYSIS OF PROTEIN PHOSPHORYLATION USING CAPILLARY ISOELECTRIC FOCUSING-ELECTROSPRAY IONIZATION MASS SPECTROMETRY

A paper submitted to Electrophoresis

Jing Wei, Liyu Yang, A. Kamel Harrata, and Cheng S. Lee[*]

Key Words: Capillary Isoelectric Focusing, Electrospray Ionization Mass Spectrometry, Protein Phosphorylation.

SUMMARY

On-line capillary isoelectric focusing (CIEF)-electrospray ionization mass spectrometry (ESIMS) as a two-dimensional separation system is employed for high resolution analysis of ovalbumin phosphorylation. On the basis of their differences in isoelectric point (pI), the mono- and diphosphoovalbumins are separated and resolved in CIEF. The focused protein zones of mono- and diphosphoovalbumins are eluted by combining gravity with cathodic mobilization. At the end of the CIEF capillary, the mobilized ovalbumin zones are analyzed by mass spectrometry coupled on-line to an electrospray interface with a coaxial sheath flow

configuration. Additional ovalbumin variants within each of mono- and diphosphoovalbumins, differing in their molecular masses due to glycosylation microheterogeneity, are easily distinguished by ESIMS.

1. INTRODUCTION

Phosphorylation has long been recognized as a reversible means of modulating protein function. By phosphorylating specific serine, threonine, and tyrosine, protein kinases alter the functions of their target proteins. Phosphorylated proteins play a critical role in transmitting extracellular signals to the nucleus. In fact, protein phosphorylation is probably the single most common intracellular signal transduction event. Among the thousands of proteins expressed in a typical mammalian cell, as many as one-third are now thought to be phosphorylated [1].

Analytical methods applied to the detection and characterization of phosphorylation sites in proteins include ^{32}P NMR, two-dimensional gel electrophoresis or complementary electrophoretic/chromatographic analysis of ^{32}P-labeled proteins with detection provided by autoradiation after exposure to X-ray films [2]. The use of immobilized metal-ion affinity chromatography to purify phosphopeptides has increased the usefulness of both matrix-assisted laser desorption/ionization mass spectrometry and liquid chromatography-electrospray ionization mass spectrometry for structural studies of protein phosphorylation [3-6]. The disadvantages of the presently used affinant, Fe^{3+}-iminodiacetic acid, are that binding to acidic peptides can occur and incomplete iron loading can result in the co-purification of His- and Lys-containing peptides.

On-line direct coupling of capillary isoelectric focusing (CIEF) with electrospray ionization mass spectrometry (ESIMS) has been demonstrated in our laboratory for the analysis of model proteins, human hemoglobin variants, bovine transferrin glycoforms, and *E. coli* proteins [7-10]. In analogy to a two-dimensional separation system, proteins are resolved in the CIEF capillary based on their differences in isoelectric point (pI). The zone sharpening effect, the characteristic of isoelectric focusing, makes CIEF a high-resolution tool for the analysis of protein variants with a pI difference as small as 0.05 pH unit. Furthermore, the focusing effect of CIEF permits the analysis of very dilute protein samples with a typical concentration factor of 50-100 times. At the end of CIEF capillary, the eluted protein zones are analyzed by mass spectrometry coupled on-line to an electrospray interface with a coaxial sheath flow configuration. ESIMS as the second dimension allows the formation of multiple-charged, high-molecular-weight ions and the precise mass determination of $\pm$ 0.01% for proteins up to 80 kDa.

In this study, on-line CIEF-ESIMS is employed for high resolution analysis of protein phosphorylation using ovalbumin as a model system. Ovalbumin has four sites of postsynthetic modification. In additional to the acetylated N-terminus, the carbohydrate moiety is located at Asn-292 and the two phosphorylated serines are at residues 68 and 344 [11]. In combination with phosphatase digestion, the distribution of molecular weight and pI of ovalbumin variants as a result of glycosylation and phosphorylation microheterogeneity is investigated using CIEF-ESIMS.

2. MATERIALS AND METHODS

Carrier ampholyte, Pharmalyte 4-6.5 was obtained from Pharmacia (Uppsala, Sweden). Chicken egg ovalbumin, 2-(N-morpholino) ethanesulfonic acid (Mes) buffer, and potato acid phosphatase were acquired from Sigma (St. Louis, MO). All other chemicals, including acetic acid, acetone, magnesium chloride, phosphoric acid, and sodium hydroxide were purchased from Fisher (Fair Lawn, NJ). All solutions were prepared using water purified by a Nanopure II system (Branstead, Dubuque, IA) and further filtered with a 0.22 mm membrane (Millipore, Bedford, MA).

2.1. Phosphatase Digestion of Ovalbumin

Ovalbumin with a concentration of 1 mM was reacted with 20 units of acid phosphatase in a 1 ml solution containing 50 mM Mes buffer and 15 mM magnesium chloride at pH 5.5. The reaction was proceeded at 37 $^{\circ}$C for various reaction times. The extent of phosphatase digestion was monitored using CIEF with UV detection.

2.2. Capillary Isoelectric Focusing: UV Measurement

The CIEF apparatus was constructed in-house using a CZE 1000R high-voltage (HV) power supply (Spellman High-Voltage Electronics, Plainview, NY) and a Linear UVIS 200 detector (Linear Instruments, Reno, NV). Fused-silica capillaries with 50 mm i.d. and 192 mm o.d. (Polymicro Technologies, Phoenix, AZ), were coated internally with linear polyacrylamide for the elimination of electroosmotic flow [12].

A 30-cm-long coated capillary was rinsed with deionized water for 2 min and was then filled with a solution containing ovalbumin and 0.5% carrier ampholyte, Pharmalyte 4-6.5. Focusing was performed by applying a constant 500 V/cm electric field across the

capillary for 15 min. The solutions of 20 mM phosphoric acid and 20 mM sodium hydroxide were used as the anolyte and the catholyte in the inlet and outlet reservoirs, respectively.

When the focusing was complete, the focused protein zones were mobilized by combining gravity with cathodic mobilization. Cathodic mobilization was initiated by replacing the sodium hydroxide catholyte with a solution containing acetone:water:acetic acid in a volume ratio of 50:49:1 at pH 2.6. To induce the gravity mobilization, the inlet reservoir was raised 8 cm above the outlet reservoir. A constant electric field of 500 V/cm was again applied during the mobilization. The protein zones were monitored by UV detector at 280 nm. The distance between the injection point and the UV detector was 24 cm.

2.3. Mass Spectrometer and Electrospray Interface

The mass spectrometer used in this study was a Finnigan MAT TSQ 700 (San Jose, CA) triple quadrupole equipped with an electrospray ionization source. The Finnigan MAT electrospray adapter kit, containing both gas and liquid sheath tubes, was used to couple CIEF with ESIMS without any modifications. The first quadrupole was used for the mass scanning of protein ions, while the second and third quadrupoles were operated in the radio-frequency-only mode. The electron multiplier was set at 1.4 kV, with the conversion dynode at -15 kV. Tuning and calibration of the mass spectrometer were established using an acetic acid solution (methanol/water/acetic acid, 50:49:1 v/v/v) containing myoglobin and a small peptide of methionine-arginine-phenylalanine-alanine.

2.4. Capillary Isoelectric Focusing-Electrospray Ionization Mass Spectrometry

For the combination of CIEF with ESIMS, a 25-cm-long coated capillary was mounted within the electrospray probe. The capillary was filled with a solution containing 0.5% Pharmalyte 4-6.5 and ovalbumin. The outlet reservoir, containing 20 mM sodium hydroxide

as the catholyte, was located inside the electrospray housing during the focusing step. The inlet reservoir, containing 20 mM phosphoric acid as the anolyte, was kept outside at the same height as the outlet reservoir. A constant voltage of 15 kV was applied during the focusing step.

Once the focusing was complete, the electric potential was turned off and the outlet reservoir was removed. The capillary tip was fixed about 0.5 mm outside the electrospray needle. A sheath liquid composed of 50% acetone, 49% water, and 1% acetic acid (v/v/v) at pH 2.6 was delivered at a flow rate of 3 ml/min using a Harvard Apparatus 22 syringe pump (South Natick, MA). During the mobilization step, two HV power supplies were used for delivering the electric potentials of 20 and 5 kV to the inlet electrode and the electrospray needle, respectively. Detailed configuration of CIEF-ESIMS including sheath liquid and electrical connections was described elsewhere [7,8].

To combine gravity with cathodic mobilizations, the inlet reservoir was raised 8 cm above the electrospray needle. No sheath gas was employed during the CIEF-ESIMS measurements. The first quadrupole was scanned from m/z 1000 to m/z 1850 at a scan rate of 1.2 sec/scan. The deconvoluted mass spectra of protein analytes were obtained using the LC/MS BioToolBox analysis software from Perkin-Elmer (Foster City, CA).

3. RESULTS AND DISCUSSION

To investigate the progress of phosphatase digestion, reaction mixtures of ovalbumin and acid phosphatase were analyzed at various reaction times using CIEF with UV detection (Fig. 1A). Two major native ovalbumin components were resolved in CIEF based on their

differences in pI. The migration time of native ovalbumin variants increased with decreasing pI value. The CIEF separation results of native ovalbumin agreed fairly well with the earlier gel electrophoresis studies [11,13], which have shown two major bands. These two electrophoresis bands were resolved on the basis of their differences in the degree of protein phosphorylation. The two major bands shown in Fig. 1A contained one and two phosphate groups and were designated as mono- and diphosphoovalbumins.

As shown in Fig. 1B-D, the CIEF separation of digestion mixture at various reaction times displayed a continuous change in the distribution of mono- and diphosphoovalbumins under the treatment with acid phosphatase. Clearly, the ratio of mono- to diphosphoovalbumins increased with increasing reaction time. At the end of 24 hours reaction time, the conversion of di- to monophosphoovalbumins was almost complete. There was no further change in the electropherogram by increasing the reaction time beyond 24 hours (data not shown).

It has been shown previously that one of the two phosphorylated sites in ovalbumin is relatively inaccessible for phosphatase action [13]. pH titration behavior indicates that both phosphoserines-68 and -344 are located on the surface of the protein. On the basis of NMR studies, phosphoserine-344 is mobile with respect to the protein surface but that phosphoserine-68 is more restricted in its motion. The phosphoserine-68 is also involved in a pH-dependent conformational change, since it is shielded from hydrolysis by phosphatase at higher pH. Furthermore, a comparison of the amino acid sequence of the phosphoserine-68 site shows that it has a striking homology to the active-site peptides of a wide variety of hydrolytic enzymes.

Two additional peaks migrating ahead of mono- and diphosphoovalbumins were observed in the electropherogram for the separation of digestion mixture at various reaction times (Fig. 1B-D). These two additional peaks were contributed by the presence of acid phosphatase in the reaction mixture and were confirmed by the analysis of phosphatase using CIEF with UV detection (data not shown).

The Pharmalyte ions similar to simpler electrolyte ions led to higher solution conductivity and contributed to the establishment of the charge excess known to exist in droplets formed during the electrospray process. Considering the effect of Pharmalyte concentration on the CIEF separation and the protein electrospray ionization mass spectra [7], a solution containing 0.5% Pharmalyte 4-6.5 and ovalbumin digestion mixture was used in the CIEF-ESIMS measurements. The reconstructed total ion electropherogram of digestion mixture at 12 hours is shown in Fig. 2. By comparing with the results shown in Fig. 1B, the increase in migration time of ovalbumin variants was attributed to the increase in the effective capillary length for the CIEF separation.

All ovalbumin variants were directly identified on the basis of mass spectra of ovalbumins taken from the average scans under the peaks. The mass spectra of mono- and diphosphoovalbumins taken from the average scans under the peaks are shown in Fig. 3A-B. Each mass spectrum displayed three major and two minor mass components. The deconvoluted molecular masses for both mono- and diphosphoovalbumins are summarized in Table 1 for comparison. A difference of 80 daltons in molecular masses further confirmed the variation in the number of phosphate groups between mono- and diphosphoovalbumin variants.

Besides the differences in the number of phosphate groups, the molecular mass differences within mono- and diphosphoovalbumin variants were contributed by glycosylation microheterogeneity at Asn-292. In fact, five groups of glycopeptides from ovalbumin under protease digestion were measured by Tai et al. [14,15] using gel filtration. The high mannose structures of ovalbumin contain various number of mannose residues in addition to a N-acetylglucosaminylb 1 - 4 N-acetylglucosamine unit linked to Asn-292. There were no attempts in this study to further characterize the carbohydrate structures associating with ovalbumin.

In conclusion, the separation of mono- and diphosphoovalbumin variants is achieved by their migration order in the CIEF separation. On the other hand, the ovalbumin variants containing the same number of phosphate groups, differing in their molecular masses due to glycosylation microheterogeneity, are easily distinguished by ESIMS. The results clearly illustrate the two-dimensional resolving power of CIEF-ESIMS for the analysis of protein phosphorylation and glycosylation in ovalbumin. The integration of CIEF with ESIMS exhibits superior resolving power, speed, and sensitivity for phosphorylation characterization in various biological and biomedical studies.

ACKNOWLEDGMENT

REFERENCES

[1]   Hubbard, M. J., Cohen, P., *Trends Biochem. Sci.* 1993, 18, 172-177.

[2]   Harrison, J. C., in Hardie, D. G. (Ed.), *Protein Phosphorylation-A Practical Approach.* Oxford University Press, New York 1992, pp. 22.

[3]   Scanff, P., Yvon, M., Pelissier, J. P., *J. Chromatogr.* 1991, 539, 425-432.

[4]   Muszynska, G., Dobrowolska, G., Medin, A., Ekman, P., Porath, J. O., *J. Chromatogr.* 1992, 604, 19-28.

[5]   Watts, J. D., Affolter, M., Krebs, D. L., Wange, R. L., Samelson, L. E., Aebersold, R., *J. Biol. Chem.* 1994, 269, 29520-29529.

[6]   Neville, D. C. A., Rozanas, C. R., Price, E. M., Gruis, D. B., Verkman, A. S., Townsend, R. R., *Protein Sci.* 1997, 6, 2436-2445.

[7]   Tang, Q., Harrata, A. K., Lee, C. S., *Anal. Chem.* 1995, 67, 3515-3519.

[8]   Tang, Q., Harrata, A. K., Lee, C. S., *Anal. Chem.* 1996, 68, 2482-2487.

[9]   Yang, L., Tang, Q., Harrata, A. K., Lee, C. S., *Anal. Biochem.* 1996, 243, 140-149.

[10]   Tang, Q., Harrata, A. K., Lee, C. S., *Anal. Chem.* 1997, 69, 3177-3182.

[11]   Nisbet, A. D., Saundry, R. H., Moir, A. J. G., Fothergill, L. A., Fothergill, J. E., *Eur. J. Biochem.* 1981, 115, 335-345.

[12]   Kilar, F., Hjerten, S., *Electrophoresis* 1989, 10, 23-29.

[13]   Vogel, H. J., Bridger, W. A., *Biochemistry* 1982, 21, 5825-5831.

[14]   Tai, T., Yamashita, K., Ogata-Arakawa, M., Koide, N., Muramatsu, T., *J. Biol. Chem.* 1975, 250, 8569-8575.

[15] Tai, T., Yamashita, K., Ito, S., Kobata, A., *J. Biol. Chem.* 1977, 252, 6687-6694.

FIGURE LEGENDS

Fig. 1   CIEF-UV detection of phosphatase digestion at (A) 0, (B) 12, (C) 18, and (D) 24

hours. Capillary, 30 cm total length/24 cm to detector, 50 mm i.d. and 192 mm o.d.;

voltage, 15 kV for focusing and mobilization; UV detection at 280 nm. The mono-

and diphosphoovalbumin variants are marked as 1 and 2, respectively.

Fig. 2   CIEF-ESIMS reconstructed total ion electropherogram of ovalbumin reaction

mixture at 12 hours after phosphatase digestion. Capillary, 25 cm total length, 50

mm i.d. and 192 mm o.d.; voltages, 15 kV for focusing and mobilization, 5 kV for

electrospray; sheath liquid, methanol/water/acetic acid (50:49:1, v/v/v) at pH 2.6, 3

ml/min; mass scan, m/z 1000 to 1850 at 1.2 sec/scan. The mono- and

diphosphoovalbumin variants are marked as 1 and 2, respectively.

Fig. 3   Positive electrospray ionization mass spectra of (A) mono- and (B)

diphosphoovalbumins taken from the average scans under the peaks in Fig. 2. The

insets present the deconvoluted molecular masses of mono- and

diphosphoovalbumin variants.

TABLE 1

Molecular Masses of Mono- and Diphosphoovalbumin Variants

Mass Component	Molecular Masses (daltons) of		Difference[a]
	Monophosphoovalbumin	Diphosphoovalbumin	
1	43,984	44,064	-80
2	44,143	44,223	-80
3	44,391	44,471	-80
4	44,596	44,676	-80
5	44,752	44,832	-80

a) Difference = molecular mass of monophosphoovalbumin - molecular mass of diphosphoovalbumin.

Figure 1

Figure 2

41
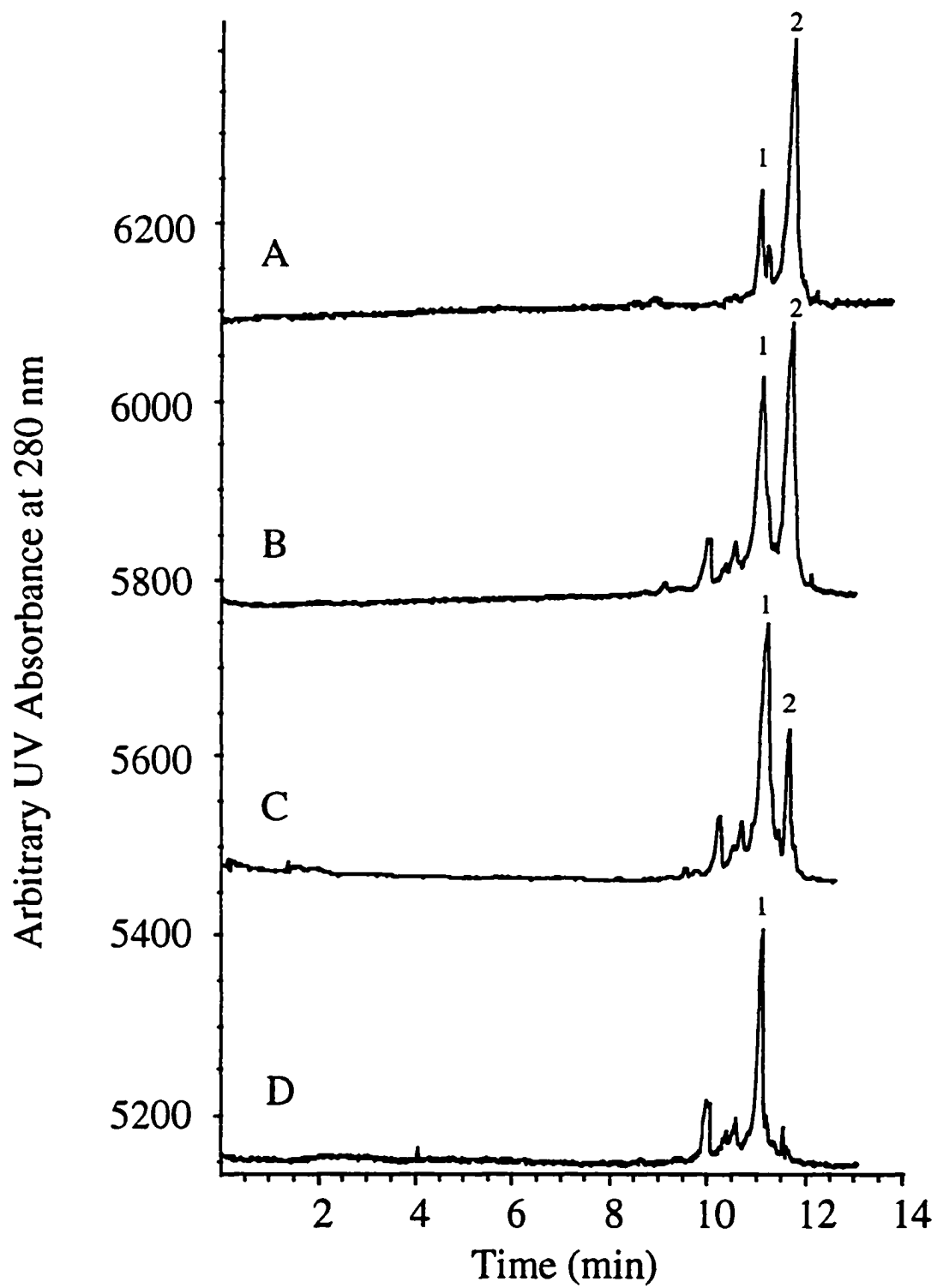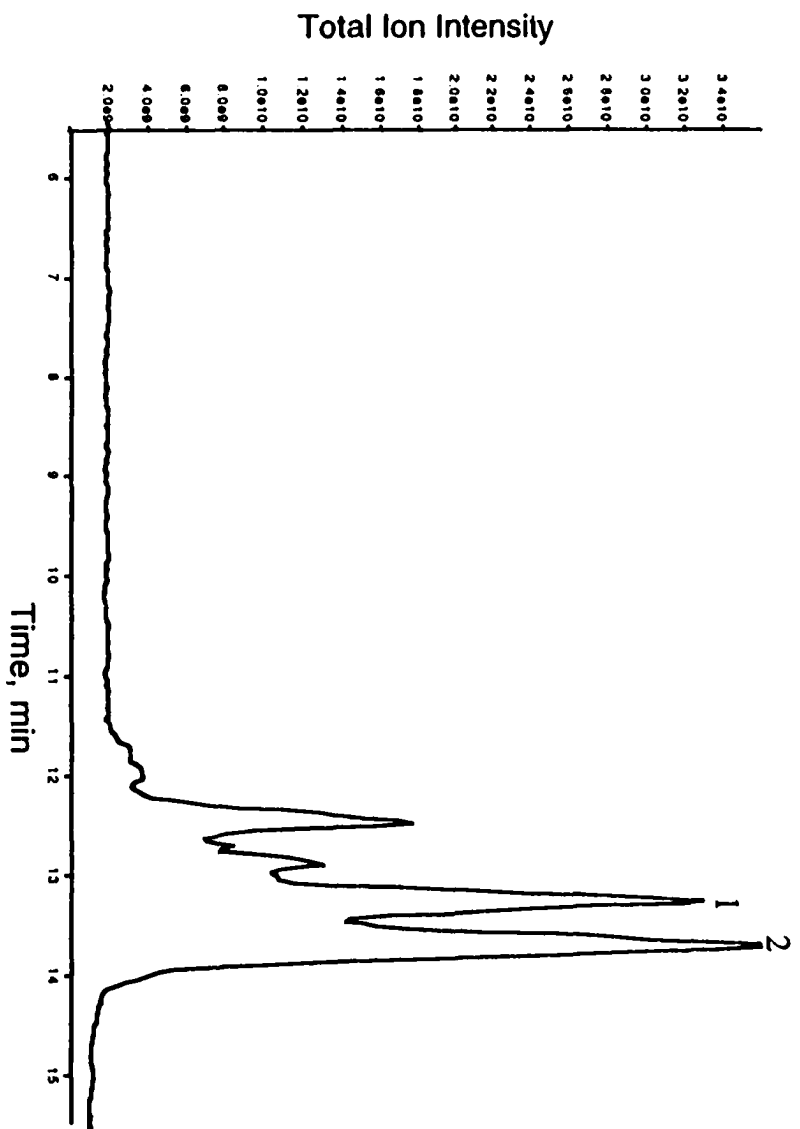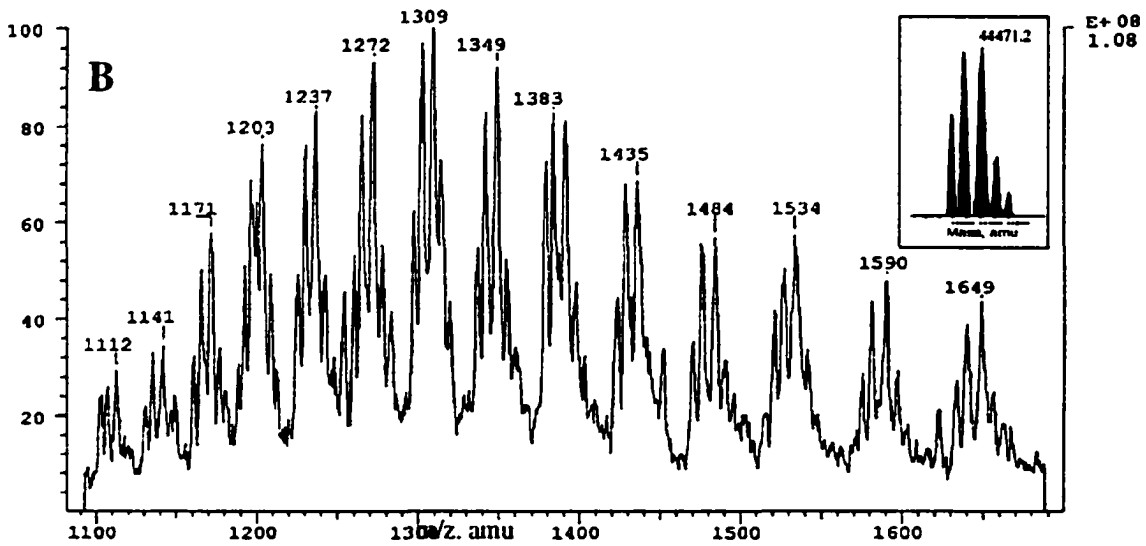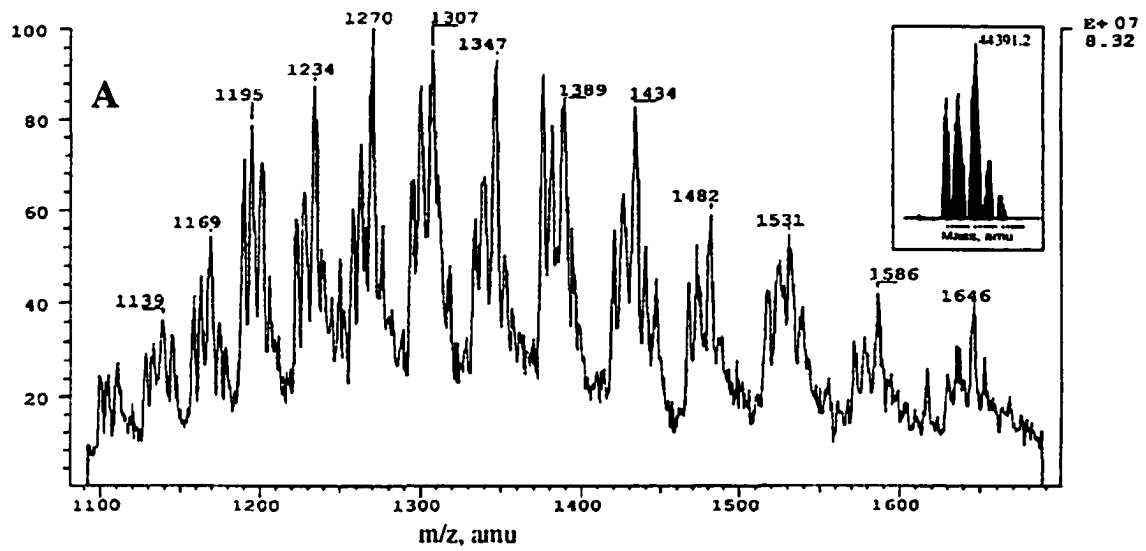
Figure 3

CAPILLARY ISOELECTRIC FOCUSING-ELECTROSPRAY IONIZATION TIME-OF-FLIGHT MASS SPECTROMETRY FOR PROTEIN ANALYSIS

A paper submitted to Microcolumn Separation

Jing Wei and Cheng S. Lee

Iulia M. Lazar and Milton L. Lee

ABSTRACT

On-line capillary isoelectric focusing (CIEF)-electrospray ionization time-of-flight mass spectrometry (ESI-TOFMS) as a two-dimensional separation system is employed for high resolution analysis of model proteins (myoglobin and b-lactoglobulin) and human hemoglobin variants C, S, F, and A. The focused proteins in a polyacrylamide-coated capillary are mobilized by replacing the sodium hydroxide catholyte with a sheath liquid solution containing methanol-water-acetic acid in a volume ratio of 80:19:1. The use of sheath liquid also establishes the electrical connection at the CIEF capillary terminus, which serves to define the electric field along the CIEF capillary and apply an electric voltage for electrospray ionization. At the end of the CIEF capillary, the mobilized protein zones are analyzed and directly identified by ESI-TOFMS. The TOFMS accumulates spectra at 5000 Hz frequency

and one averaged spectrum is acquired per second during the CIEF-ESI-TOFMS measurements.

Key Words: Capillary Isoelectric Focusing, Electrospray Ionization, Time-of-Flight Mass Spectrometry.

INTRODUCTION

The traditional biochemical approach to protein characterization has been the use of two-dimensional gel electrophoresis[1]. Despite the selectivity and sensitivity of two-dimensional gel electrophoresis, this technique as practiced today is a collection of manually intensive procedures. Casting of gels, application of samples, running of gels, and staining of gels are all time-consuming tasks, prone to irreproducibility and poor quantitative accuracy.

In capillary isoelectric focusing (CIEF), the fused-silica capillary contains not only ampholytes but also proteins[2-4]. When an electric potential is applied, the negatively charged acidic ampholytes migrate toward the anode and decrease the pH at the anodic section, while the positively charged basic ampholytes migrate toward the cathode and increase the pH at the cathodic section. Protein analytes as amphoteric macromolecules also focus at their pI values in narrow zones in the same way as the individual ampholytes. The focusing effect of CIEF permits analysis of dilute protein samples with a typical concentration factor of 50-100 times.

In analogy to two-dimensional gel electrophoresis, on-line combination of CIEF with electrospray ionization mass spectrometry (ESIMS) has been demonstrated for the analysis of human hemoglobin variants[5], bovine transferrin glycoforms[6], and recombinant E. coli proteins[7]. The scan rate of quadrupole mass spectrometers, however, may be insufficient to truly reflect the excellent separation efficiency of CIEF. An alternative strategy is to use multichannel detection such as array detection in time-of-flight mass spectrometry (TOFMS) to acquire a complete mass spectrum for each time interval over the course of a CIEF peak.

On-line interfacing of capillary zone electrophoresis (CZE) to TOFMS has been recently reported using ESI sources[8-13]. Along with speed, other advantages of TOFMS include unlimited mass range, high ion transmission efficiency, high duty cycle, sensitivity, and simplicity. In this study, we report the on-line combination of CIEF with TOFMS using an ESI source for various protein analyses. The proteins are focused and mobilized in a polyacrylamide-coated capillary. At the end of the CIEF capillary, the mobilized protein zones are analyzed by ESI-TOFMS using a coaxial sheath flow configuration. The use of sheath flow establishes the electrical connection at the CIEF capillary terminus, which serves to define the electric field along the CIEF capillary and apply an electric voltage for electrospray ionization[14].

EXPERIMENTAL

Reagents

Standard proteins including myoglobin (horse heart, 16,951 daltons, pI 7.2 and 6.8) and b-lactoglobulin (bovine milk, 18,363 daltons, pI 5.1) were purchased from Sigma (St. Louis, MO). Human hemoglobin variants C, S, F, and A were obtained from Isolab (Akron, OH). All chemicals, including acetic acid, methanol, phosphoric acid, and sodium hydroxide, were

purchased from Fisher (Fair Lawn, NJ). All solutions were filtered through a 1-mm filter (Whatman, Maidstone, England).

Electrospray Interface and Time-of-Flight Mass Spectrometer

A home-built electrospray interface (see Fig. 1) was used to combine CIEF on-line with TOFMS. The electrospray voltage was maintained around 3 kV and was applied to the nebulizing tubing and the electrospray needle. The electrical contact at the CIEF capillary terminus was established through the use of a sheath liquid. A microscope (Edmund Scientific, Barrington, NJ) positioned in front of and at an oblique angle above the electrospray source permitted the adjustment of the capillary tip outside the electrospray needle and the evaluation of the spray characteristics. A fiberoptic illuminator (Edmund Scientific) was used to shine light over the spray.

The TOF mass spectrometer was constructed in-house and described elsewhere[13]. The TOFMS consisted of an ion source and four differentially pumped vacuum stages. A countercurrent of hot nitrogen gas allowed for the drying of the electrosprayed ions, protected the nozzle, and maintained a clean atmosphere in the source. The association of the high-efficiency focusing capacities of the quadrupole with the high-speed characteristics of the TOF analyzer led to the ideal mass spectrometer detector, essential for the analysis of proteins resolved in CIEF. Tuning and calibration of the mass spectrometer were established using an acetic solution (methanol/water/acetic acid, 80:19:1 v/v/v) containing myoglobin.

Capillary Isoelectric Focusing-Electrospray Ionization Time-of-Flight Mass Spectrometry

Fused silica capillaries, 50 mm i.d. and 192 mm o.d. (Polymicro Technologies, Phoenix, AZ), were coated internally with linear polyacrylamide for the elimination of electroosmotic flow and protein adsorption onto the capillary wall[4]. A 30-cm-long CIEF capillary was filled with a solution containing proteins and carrier ampholyte, pharmalyte 3-10 or 5-8 (Pharmacia, Uppsala, Sweden). For the combination of CIEF with ESI-TOFMS, the capillary was mounted within the electrospray probe. The outlet reservoir, containing 20 mM sodium hydroxide as the catholyte, was located on the interface plate (see Fig. 1) during the focusing step. The inlet reservoir, containing 20 mM phosphoric acid as the anolyte, was kept outside the electrospray housing at the same height as the outlet reservoir. Focusing was performed at a 15-kV constant voltage for 10 min.

Once the focusing was complete, the electric potential was turned off, and the outlet reservoir was removed. The position of the capillary tip in the electrospray needle was adjusted under the microscope for obtaining a stable spray current. The sheath liquid consisted of 80% methanol, 19% water, and 1% acetic acid (v/v/v) at pH 2.6 and was delivered at a flow rate of 2.3 mL min^{-1} with the use of a Harvard 22 syringe pump (South Natick, MA). During the mobilization step, two CZE 1000R high-voltage power supplies (Spellman High-Voltage Electronics, Plainview, NY) were used for delivering the electric potentials of 18 kV and 3 kV at the inlet electrode and the electrospray needle, respectively. To combine gravity with cathodic mobilization, the inlet reservoir was raised 8 cm above the electrospray needle. No sheath gas was employed during the CIEF-ESI-TOFMS measurements.

RESULTS AND DISCUSSION

Considering the effects of ampholyte concentration on the CIEF separation and the protein electrospray ionization mass spectra[15], a solution containing 0.5% pharmalyte 3-10 and model proteins was used in the CIEF-ESI-TOFMS measurements. To prevent the carrier ampholytes from migrating into the inlet and outlet reservoirs by diffusion during the focusing step, 20 mM phosphoric acid and 20 mM sodium hydroxide solutions were used as the anolyte and the catholyte, respectively. Once the focusing was complete, the focused protein zones were then mobilized by replacing the sodium hydroxide catholyte with a sheath liquid solution containing methanol-water-acetic acid in a volume ratio of 80:19:1.

In order to maintain electroneutrality during electrophoretic separation, the electric charge transported by the ions exiting one end of the CIEF capillary must be substituted by a charge carried by ions of the same sign entering the opposite end of the capillary. For the capillaries with limited or zero electroosmotic flow (such as the polyacrylamide-coated tubing), the sheath liquid counterions used in the electrospray interface migrate into the CIEF capillary, replacing the original counterions of the background electrolyte[5,16,17]. In this study, the formation of a moving acetate ion boundary from the sheath liquid was minimized by introducing a gravity-induced hydrodynamic flow together with cathodic mobilization of the focused protein zones in the CIEF capillary.

As shown in Fig. 2, the elution order was myoglobin (pI 7.2 and 6.8), followed by b-lactoglobulin (pI 5.1). The differences in the migration times between the protein peaks during cathodic mobilization did not truly correspond to their differences in pI values. The non-linear velocity gradient during cathodic mobilization resulted in a greater separation among basic proteins than that of acidic proteins with similar pI difference.

All protein peaks were directly identified on the basis of averaged mass spectra of protein analytes taken under the peaks. An example of an averaged mass spectrum obtained under the peak of myoglobin (pI 7.2) is shown in Fig. 3. The peak with a flight time of 52.94 ms corresponded to myoglobin ions with m/z of 997.12. The deconvoluted masses of myoglobin and b-lactoglobulin measured from the electrospray mass spectra are summarized in Table I. A relative standard deviation of 0.01-0.03% between the expected and measured molecular masses of model proteins was demonstrated for precise mass determination.

To date, the high-speed data acquisition system produces sufficient noise to require a relatively high number of spectra to be averaged to obtain a clean spectrum. The TOFMS accumulated spectra at 5000 Hz frequency and one averaged spectrum was acquired per second during the CIEF-ESI-TOFMS measurements. Thus, an acquisition rate of one data point per second (5000 Hz pulsing rate, 5000 averaged spectra per data point) would be sufficient for accurately monitoring the CIEF protein separation. In comparison with CIEF-UV measurements (data not shown), the additional downtime needed for removing the outlet reservoir and positioning the capillary tip outside the electrospray needle between the focusing and mobilization steps might contribute to a possible source of peak broadening in CIEF-ESI-TOFMS. In our previous studies[5-7,15,17], the whole procedure for removing the outlet reservoir and for positioning the capillary tip in the Finnigan CE-MS electrospray interface was done in less than 1 min. However, it took about 10 min to complete the whole procedure and obtain a stable spray current in a home-built electrospray interface (see Fig. 1).

A solution containing 0.5% pharmalyte 5-8 and human hemoglobin variants with a total concentration of 1 mg mL^{-1} was employed in the CIEF-ESI-TOFMS measurements. The reconstructed ion electropherogram of hemoglobin variants C (pI 7.5), S (pI 7.25), F (pI 7.15)

and A (pI 7.10) is shown in Fig. 4. In CIEF-UV measurements (data not shown), hemoglobin variants F and A, the wild type fetal and adult hemoglobins, were baseline separated and resolved with a pI difference of 0.05 pH units. Again, the additional downtime during the focusing and mobilization steps resulted in loss of separation efficiency and resolution of hemoglobin variants in CIEF-ESI-TOFMS.

All hemoglobin variants were directly identified on the basis of the averaged mass spectra of hemoglobins taken under the peaks. An example of an averaged mass spectrum obtained under the peak of hemoglobin S (pI 7.25) is shown in Fig. 5. Two separate electrospray ionization envelopes with different ion intensities were observed for the a and b^S chains. The mass resolution of the linear TOFMS used in this study was only around 400, however, the use of a reflectron design[12] would clearly offer better resolution between the a and b^S chains. The presence of two electrospray envelopes indicated the dissociation of the hemoglobin S tetramer due to heating and/or collisional excitation in the interface region. The deconvoluted masses of the hemoglobin chains measured from the electrospray mass spectra are summarized in Table I. A relative standard deviation of 0.03-0.04% between the expected and measured molecular masses of the hemoglobin chains was demonstrated for precise mass determination.

ACKNOWLEDGMENTS

REFERENCES

1. *Protein Structure: A Practical Approach*, T. E. Creighton (IRL Press, New York, 1990), Chapter 3.

2. S. Hjerten and M. D. Zhu, *J. Chromatogr.* **346**, 265 (1985).

3. S. Hjerten, J. L. Liao, and J. Yao, *J. Chromatogr.* **387**, 127 (1987).

4. F. Kilar and S. Hjerten, *Electrophoresis* **10**, 23 (1989).

5. Q. Tang, A. K. Harrata, and C. S. Lee, *Anal. Chem.* **68**, 2482 (1996).

6. L. Yang, Q. Tang, A. K. Harrata, and C. S. Lee, *Anal. Biochem.* **243**, 140 (1996).

7. Q. Tang, A. K. Harrata, and C. S. Lee, *Anal. Chem.* **69**, 3177 (1997).

8. L. Fang, R. Zhang, E. R. Williams, and R. N. Zare, *Anal. Chem.* **66**, 3696 (1994).

9. D. C. Muddiman, A. L. Rockwood, Q. Gao, J. C. Severs, H. R. Udseth, and R. D. Smith, *Anal. Chem.* **67**, 4371 (1995).

10. J. F. Banks and T. Dresch, *Anal. Chem.* **68**, 1480 (1996).

11. J.-T. Wu, M. G. Qian, M. X. Li, L. Liu, and D. M. Lubman, *Anal. Chem.* **68**, 3388 (1996).

12. M. X. Li, L. Liu, J.-T. Wu, and D. M. Lubman, *Anal. Chem.* **69**, 2451 (1997).

13. I. M. Lazar, B. Xin, M. L. Lee, E. D. Lee, A. L. Rockwood, J. C. Fabbi, and H. G. Lee, *Anal. Chem.* **69**, 3205 (1997).

14. R. D. Smith, J. H. Wahl, D. R. Goodlett, and S. A. Hofstadler, *Anal. Chem.* **65**, 574A (1993).

15. Q. Tang, A. K. Harrata, and C. S. Lee, *Anal. Chem.* **67**, 3515 (1995).

16. F. Foret, T. J. Thompson, P. Vouros, B. L. Karger, P. Gebauer, and P. Bocek, *Anal. Chem.* **66**, 4450 (1994).

17. Q. Tang, A. K. Harrata, and C. S. Lee, *J. Mass Spectrom.* **31**, 1284 (1996).

18. R. D. Smith, J. A. Loo, C. G. Edmonds, C. J. Barinaga, and H. R. Udseth, *Anal. Chem.* **62**, 882 (1990).

19. F. Foret, O. Muler, J. Thorne, W. Gotzinger, and B. L. Karger, *J. Chromatogr. A* **716**, 157 (1995).

20. *Mass Spectrometry: Clinical and Biomedical Applications*, C. H. L. Shackleton and H. E. Witkowska (Plenum Press, New York, 1994), Volume 2, Chapter 4.

FIGURE LEGENDS

Fig. 1   Schematic diagram of the electrospray interface. (1) Electrospray chamber 1-T; (2) electrospray chamber 2; (3) electrospray needle, 26 gauge; (4) nebulizing tubing-stainless steel; (5) make-up gas tubing-glass; (6) CIEF capillary; (7) Teflon T-union; (8) nuts, tubing connectors; (9) interface; (10) nozzle.

Fig. 2   CIEF-ESI-TOFMS reconstructed ion electropherogram of 0.5 mg ml^{-1} each of (1) myoglobin (pI 7.2), (2) myoglobin (pI 6.8), and (3) b-lactoglobulin (pI 5.2). Capillary, 30 cm total length, 50 mm i.d. and 192 mm o.d.; carrier ampholyte, 0.5% pharmalyte 3-10; applied voltages, 15 kV for focusing and mobilization, 3 kV for electrospray; sheath liquid, methanol/water/acetic acid (80:19:1 v/v/v) at pH 2.6, 2.3 ml min^{-1}.

Fig. 3   Positive ion electrospray mass spectrum taken under the peak of myoglobin (pI 7.2) in Fig. 2.

Fig. 4   CIEF-ESI-TOFMS reconstructed ion electropherogram of human hemoglobin variants with a total concentration of 1 mg ml^{-1}. Carrier ampholyte, 0.5% pharmalyte 5-8. Other conditions were the same as in Fig. 2.

Fig. 5   Positive ion electrospray mass spectrum taken under the peak of hemoglobin S in Fig. 4.

TABLE I

Molecular Weights of Model Proteins and Various Hemoglobin Chains

Protein/ Hemoglobin Chain	Measured Molecular Weight (Daltons)	Expected Molecular Weight (Daltons)[a]	Relative Error (%)
Myoglobin	16,953	16,951	+0.01
b-lactoglobulin	18,368	18,363	+0.03
a	15,120	15,126	-0.04
b^A	15,862	15,867	-0.03
b^C	15,862	15,866	-0.03
b^S	15,831	15,837	-0.04
g	15,991	15,995	-0.03

a) From references (18-20).

Schematic Diagram of the Electrospray Interface
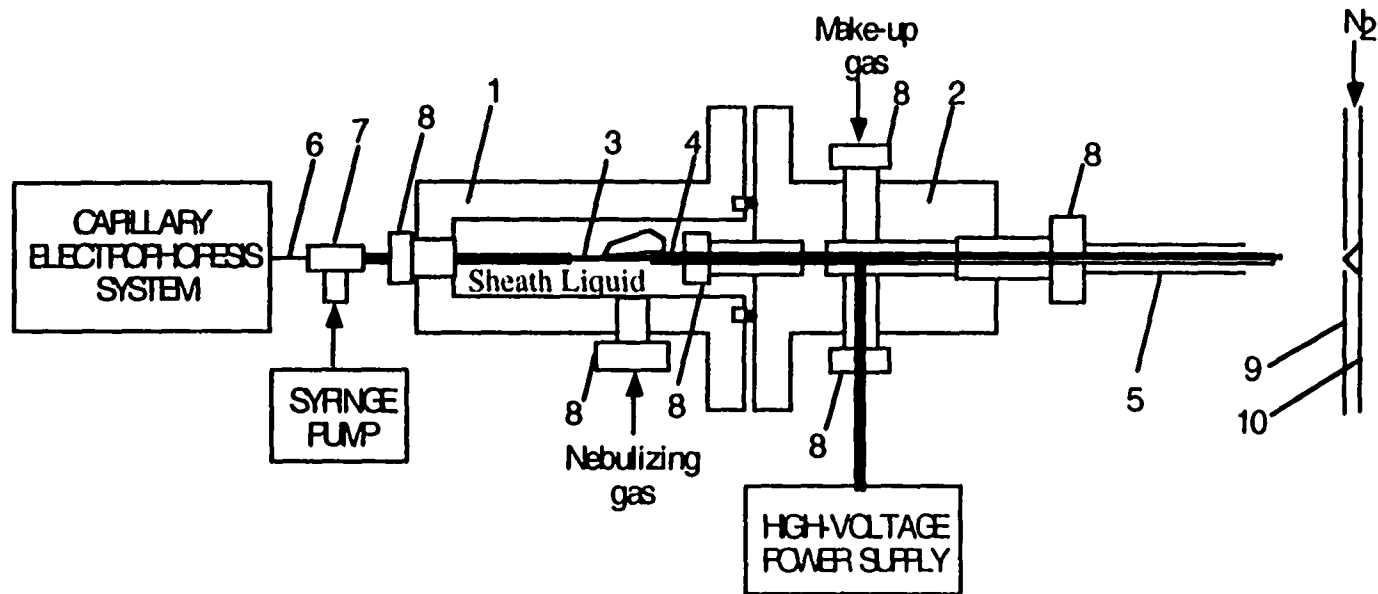
Figure 1. (1) Electrospray chamber 1-T; (2) electrospray chamber 2; (3) electrospray needle, 26 gauge; (4) nebulizing tubing-stainless steel; (5) make-up gas tubing-glass; (6) CIEF capillary; (7) Teflon T-union; (8) nuts, tubing connectors; (9) interface; (10) nozzle.
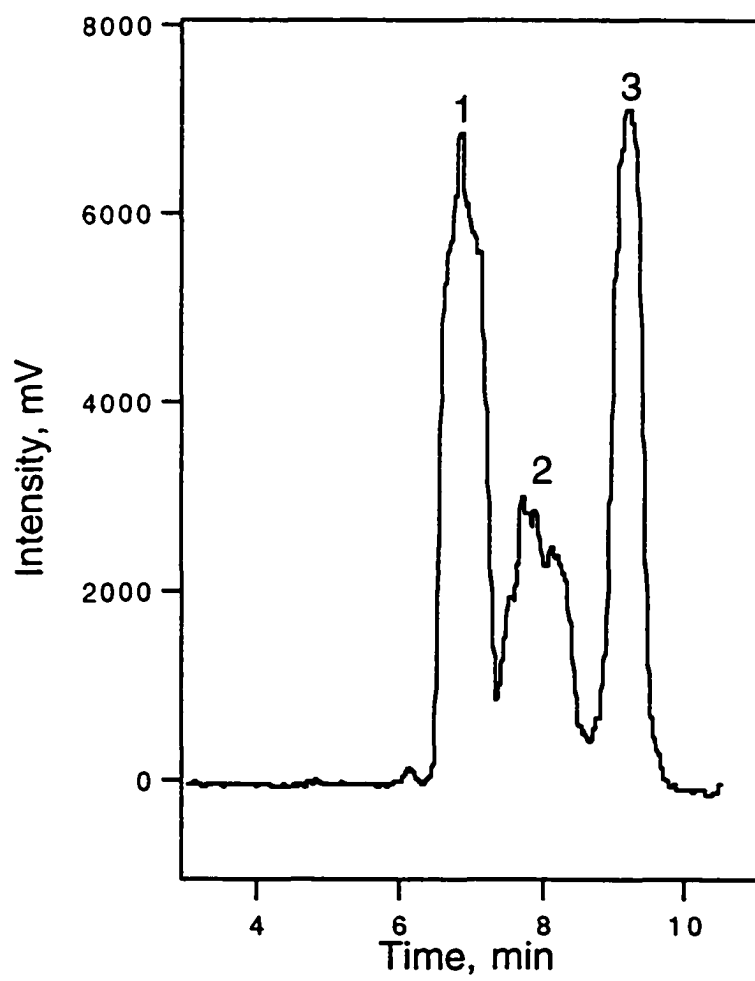
Figure 2
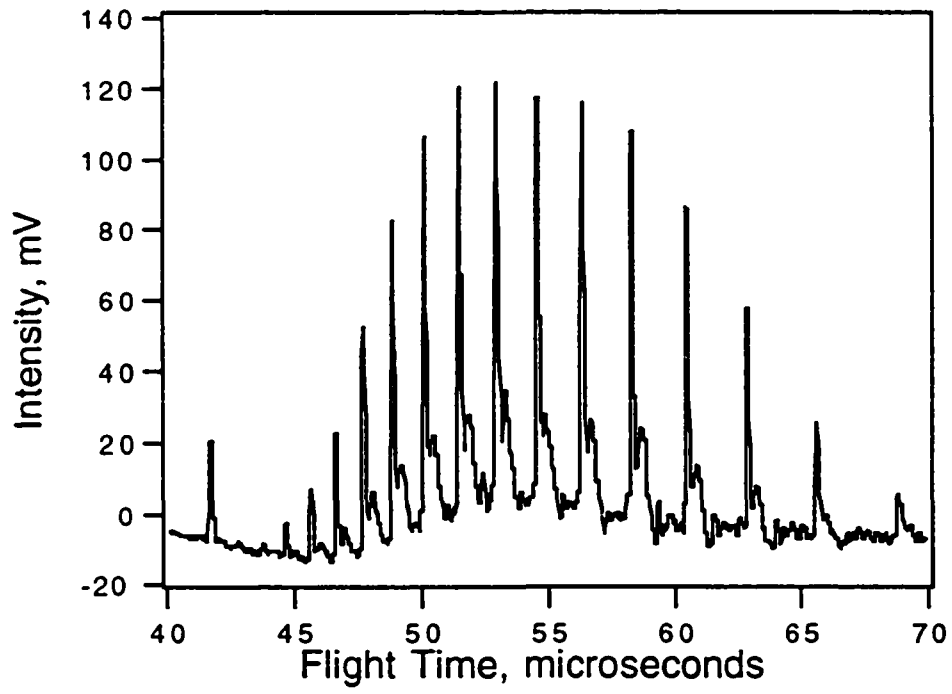
Figure 3
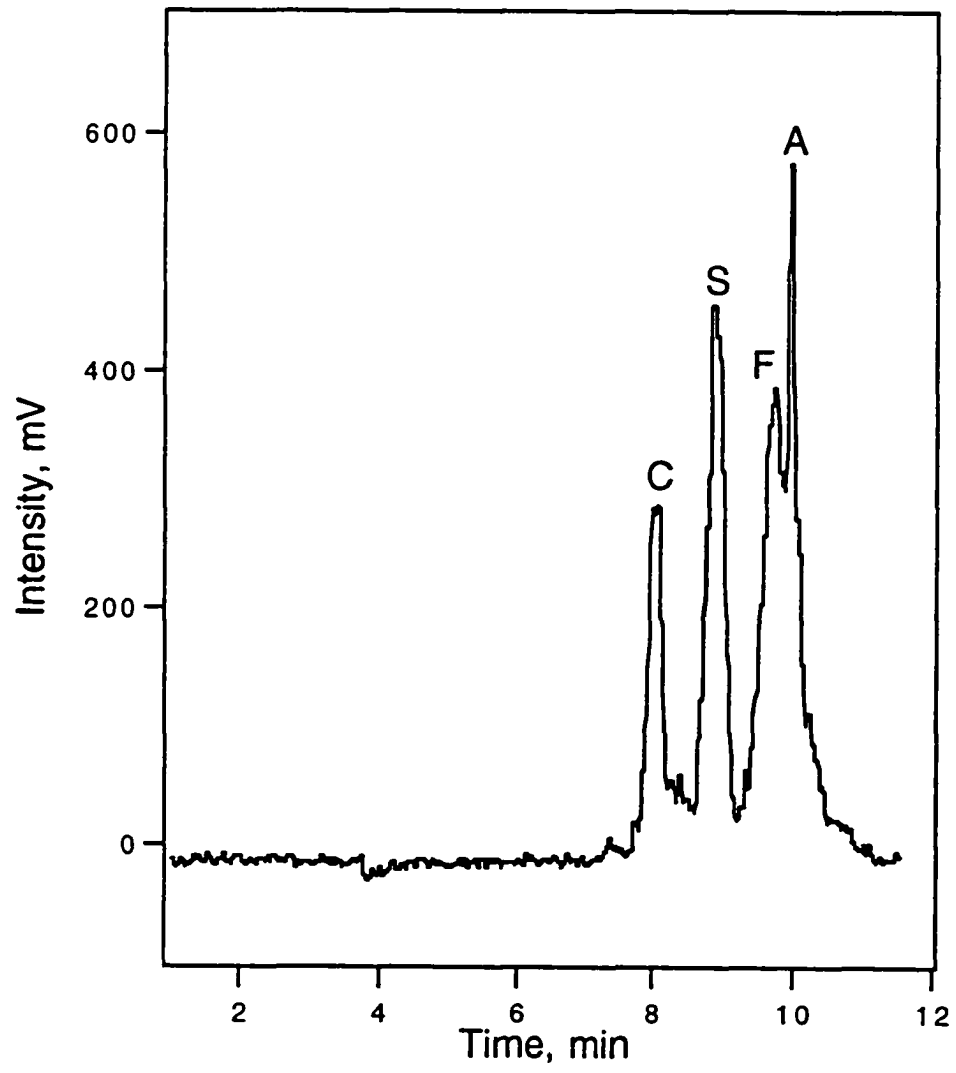
Figure 4
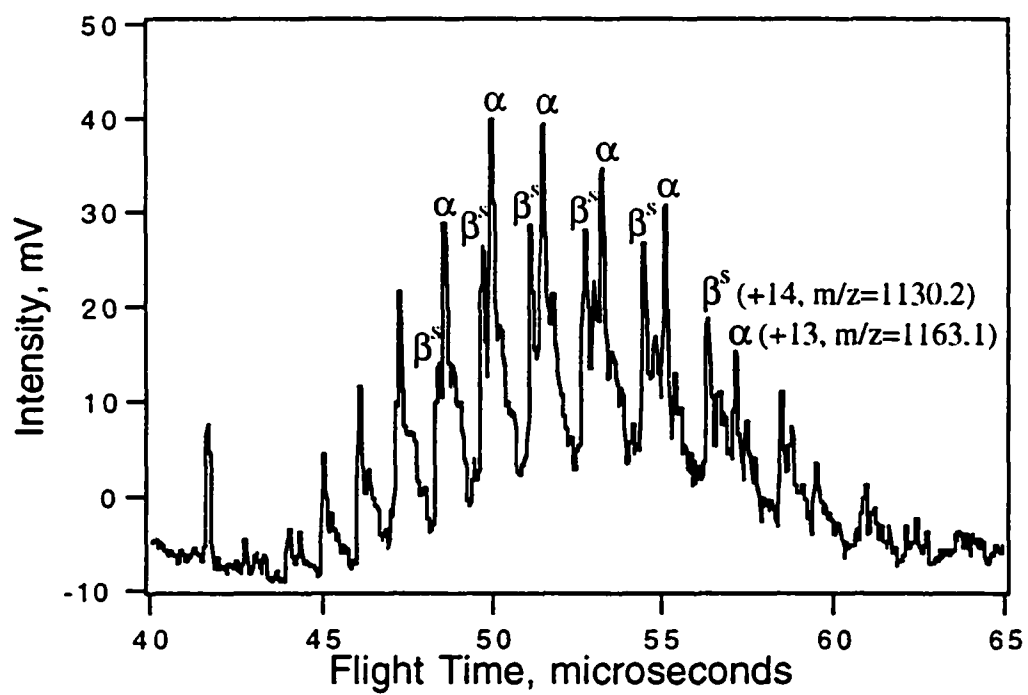
Figure 5

ON-LINE COUPLING OF CAPILLARY ISOELECTRIC FOCUSING AND LIQUID CHROMATOGRAPHY WITH ELECTROSPRAY MASS SPECTROMETRY FOR CHARACTERIZATION OF PHOSPHORYLATION OF PHOSPHO-TAU PROTEIN

A paper prepared for submission to Bioanalytical Chemistry

Jing Wei, and Cheng S. Lee

Huang-Chun Tseng, and Donald J. Graves

A. Kamel Harrata

ABSTRACT

A recombinant tau expressed in *E. Coli* was phosphorylated by two different kind of protein kinases: cAMP-dependent protein kinase A (PKA) and microtubule binding repeat kinase (MBR) purified from rat brain. At the protein level, a comparison of tau proteins

before and after controlled PKA phosphorylation is carried out using capillary isoelectric focusing-electrospray ionization mass spectrometry (CIEF-ESI MS). Phosphorylation by PKA increased the retention time and the molecular mass of tau protein, and lowered the pI value.

The phospho-taus were studied at the peptide level by a combination of reversed-phase liquid chromatography-electrospray ionization mass spectrometry (LC-ESI MS) and LC-ESI MS/MS by neutral loss detection[Covey, 1991 #10]. The condition of LC-ESI neutral loss MS/MS is improved and optimized using a model phospho- and dephospho-peptide mixture. Good sensitivity is obtained and detection of sub-picomole amounts of phosphopeptides is presented. Phosphopeptides were selectively detected by LC-ESI neutral loss MS/MS in which the characteristic neutral loss of phosphoric acid from phosphopeptides by collision-induced dissociation (CID) conditions. Informative RIC of ESI neutral loss MS/MS is reported for the detection of phosphopeptide in tryptic digest. M/z values were obtained and an equation is suggested for the possible charged state determination. Based on m/z value and reproducible retention times of phosphopeptides from LC-ESI MS RIC profiles, complimentary information was obtained which allows us to confirm the identity and number of phosphorylation sites. Four and five phosphorylation sites were identified for PKA phospho-tau and MBR kinase phospho-tau, respectively. A quantitative methodology was suggested for the determination of phosphorylation stoichoimetry based on ion intensities from RIC of LC-ESI MS.

INTRODUCTION

Phosphorylation has long been recognized as a reversible means of modulating protein function. By phosphorylating specific serine, threonine, and tyrosine, protein kinases alter the functions of their target proteins. Phosphorylated proteins play a critical role in transmitting extracellular signals to the nucleus. In fact, protein phosphorylation is probably the single most common intracellular signal transduction event. Among the thousands of proteins expressed in a typical mammalian cell, as many as one-third are now thought to be phosphorylated(1).

Tau, a microtubule-associated protein, is abnormally phosphorylated in Alzheimer's disease (AD) brain. Tau proteins are extended, microtubule-associated proteins with little or no secondary structures(2). In human brain there are six known tau isoforms(3). All these forms contain three or four imperfect tandem repeats in the carboxyl half of the molecule, and either no, one or two inserts in the N-terminal portion. Paired helical filaments (PHFs), which are abnormal fibrous structures found in brains of patients with Alzheimer's disease, are composed primarily of all six brain tau forms in a hyperphosphorylated state (PHF-tau)(4-6). It was suggested that hyper-phosphorylation of tau causes loss of tau's biological function through loss its binding ability to microtubule and leads to neuronal damage(5). The number and location changes of the phosphorylation on tau protein are closely related to the severity of the disease. We use the recombinant tau phosphorylated by different kinases to

establish some approaches for high resolution phosphorylation characterization and kinase specificity determination, upon which tau from normal or patient brains can be studied for pursuing the diagnosis and treatment of Alzheimer's disease.

Analytical methods applied to the detection and characterization of phosphorylation sites in proteins include ^{32}P NMR, amino acid sequencing by Adam degradation, two-dimensional gel electrophoresis or complementary electrophoretic/chromatographic analysis of ^{32}P-labeled proteins with detection provided by autoradiation after exposure to X-ray films(7).

On-line direct coupling of capillary isoelectric focusing (CIEF) with electrospray ionization mass spectrometry (ESIMS) has been demonstrated in our laboratory for the analysis of model proteins, human hemoglobin variants, bovine transferrin glycoforms, and E. coli proteins (8-11). In analogy to a two-dimensional separation system, proteins are resolved in the CIEF capillary based on their differences in isoelectric point (pI). The zone sharpening effect, the characteristic of isoelectric focusing, makes CIEF a high-resolution tool for the analysis of protein variants with a pI difference as small as 0.05 pH unit. Furthermore, the focusing effect of CIEF permits the analysis of very dilute protein samples with a typical concentration factor of 50-100 times. At the end of CIEF capillary, the eluted protein zones are analyzed by mass spectrometry coupled on-line to an electrospray interface with a coaxial sheath flow configuration. ESIMS as the second dimension allows the formation of multiple-charged, high-molecular-weight ions and the precise mass determination of $\pm$ 0.01% for proteins up to 80 kDa. ESI MS was employed for the elucidation of the

difference in mass of the phosphorylated and dephosphorylated protein forms. Knowledge of the difference in mass and the assumption that both forms are homogenous enables an approximate determination of the phosphorylation state in the phosphoproteins. In this study, on-line CIEF-ESIMS is employed for high resolution analysis of tau phosphorylation for both determination of pI and number of phosphorylation site.

Matrix-assisted laser desorption mass spectrometry has been used to determine phosphopeptides as masses with 80-Da increments greater than the predicted peptide molecular weights(12-15); However, to combine the separation techniques such as capillary electrophoresis or HPLC with MALDI, off-line coupling is the only choice at the current stage. ESI-MS combined with RP/HPLC provides an alternative to the conventional mapping procedure for the location of phosphopeptides(16,17). Peptide mapping by mass spectrometry has emerged as a powerful tool for the characterization of phosphoproteins. A comparison of the proteolytic digest of phosphorylated or non-phosphorylated protein by LC/MS facilitates the identification of modified peptides. However, peptide mapping by comparison of reconstructed ion current chromatogram (RIC) profiles is rather laborious process, requiring knowledge of the amino acid sequence of the protein. Application to unknown or novel proteins would therefore not be fully effective, so methods are pursued to selectively isolate phosphopeptides from the background digest. ESI-MS is able to detect phosphopeptides specifically by tandem MS (MS/MS). The characteristic neutral loss of phosphoric acid of phosphopeptides by collision-induced dissociation (CID) condition has been exploited to highlight phosphopeptides in a peptide mixture(17,18). Phosphopeptides

with major phospho-sites were identified by direct infusion neutral-loss MS/MS at m/z 49 in

a_{s1}-casein tryptic digest(18). However, since m/z is the only information for the

identification of peptides and one m/z value may fit for more than one tryptic

phosphopeptides, it could be difficult to draw any conclusion. On-line coupling of LC with

neutral loss MS/MS provides the separation in the digestion mixture, and gives simpler

spectra from separated peaks with better sensitivity than the direct infusion due to the low

background noise. Furthermore, the information provided by the LC separation (e.g.

separation time) can help locate the phosphopeptides in total peptide mapping where

additional information can be drawn to further characterize the phosphorylation. However,

earlier attempts using this protocol gave only poor response (18), and even less information

was obtained by on-line coupling LC-ESI neutral loss MS/MS than by direct infusion.

By neutral loss monitoring at m/z 49, it was thought the detected peptide ions were

only the doubly charged phosphopeptides and fit to the equation: neutral loss = 98/n (n =

number of charges)(19). However, we found the detected ions include not only the doubly

charged phosphopeptide (loss of one phosphate group) but also other multiple charged

peptide ions (loss of more than one phosphate group), for example, fourfold charged

diphosphopeptide with the loss of both phosphates. A more complete equation is suggested

and used for charged state determination in our study.

The first step of our study is to improve and optimize the condition of LC-ESI neutral

loss MS/MS by using a model phospho- and dephospho- peptide mixture. The utility of this

method for the detection of sub-picomole amounts of phosphopeptides is presented. From

LC neutral loss MS/MS, reproducible LC retention time helps locate the phosphopeptides in LC-ESI MS RIC profiles. Thus some complimentary information was obtained to confirm and further characterize the identity and number of phosphorylation sites. The combination of LC-ESI MS and LC-ESI neutral loss MS/MS is applied to tryptic digest of phosphotau to study its phosphorylation at the peptide level. Selective identification of phosphopeptide was carried out by LC-ESI MS/MS in the neutral loss mode, and detailed studies of peptide maps were based on RIC of LC-ESI MS. Phosphorylation sites of PKA and MBR kinase on recombinant tau were detected and identified. We also suggest a quantitative method for the determination of stoichoimetry of phosphorylation.

MATERIALS AND METHODS

Materials

Tau phosphopeptides and their dephosphorylated analogs were synthesized by Protein Facility at Iowa State University and are listed in Table I.

Carrier ampholyte, pharmalyte 3-10 was obtained from Pharmacia (Uppsala, Sweden). cAMP-dependent protein kinase A (PKA) was from Promega (Madison, Wisconsin). Trypsin (sequencing grade), trifluoroacetic acid (TFA), the model proteins, including cytochrome C, myoglobin (horse heart) and carbonic anhydrase I were obtained from Sigma

(St. Louis, MO). All other chemicals and reagents were purchased from Fisher (Fair Lawn, NJ) or Sigma.

Expression, Purification, *in vitro* Phosphorylation, and Trytic Digestion of the Longest Human Tau Protein

The bacteria plasmid cloned with longest human tau protein cDNA was transformed into *Escherichia coli* BL 21 (DE 3). Cells were grown in ampicillin-containing LB media at 37°C with 250rpm shaking. Expression of tau protein was induced with the addition of 0.4 mM IPTG when OD of cells at 600 nm reached 0.6. Cells were harvested with low speed centrifugation after 5 hour induction, suspended in pH 6.8 buffer, and broken by cycle sonication. Cell homogenate supernatant was heated at 95°C for 5 min. After removal of aggregate, tau was further purified by SP-sepharose chromatography with increasing salt concentration and followed by HPLC. The biological activity of tau was verified with *in vitro* microtubule assembly test.

The phosphorylation reaction mixture contains 20 mM recombinant tau, either 10 units of PKA or certain amount of MBR kinase, 1 mM $MgCl_2$, 1 mM ATP, 1 mM DTT, 0.2 mM microcystin-LR, protease inhibitors and 12.5 mM Tris/12.5 mM Hepes, pH 7.5. Reaction mixtures were incubated in a 30°C water bath for 18 hours and terminated by heating at 95°C for 10 min. Precipitated proteins were removed by 0.22 mm filtration. For tryptic digestion, the filtrate was incubated with trypsin at 2% the weight of total tau for 4 hours at 37°C. An

additional trypsin portion was added and incubated continually for another 4 hours. Trypsin digestion was stopped by heating at 95°C for 10 min followed by removal precipitate as described above.

Mass Spectrometer and Electrospray Interface

The mass spectrometer used in this study was a Finnigan MAT TSQ 700 (San Jose, CA) triple quadruple equipped with an electrospray ionization source. The Finnigan MAT electrospray adapter kit, containing both gas and liquid sheath tubes, was used to couple CIEF with ESIMS without any modifications. The first quadruple was used for the mass scanning of protein ions, while the second and third quadruples were operated in the radio-frequency-only mode. The electron multiplier was set at 1.4 kV, with the conversion dynode at -15 kV. Tuning and calibration of the mass spectrometer were established using an acetic acid solution (methanol/water/acetic acid, 50:49:1 v/v/v) containing myoglobin and a small peptide of methionine-arginine-phenylalanine-alanine.

Capillary Isoelectric Focusing-Electrospray Ionization Mass Spectrometry

For the combination of CIEF with ESIMS, a 25-cm-long capillary was mounted within the electrospray probe. Fused-silica capillaries with 50 mm i.d. and 192 mm o.d. (Polymicro

Technologies, Phoenix, AZ), were coated internally with linear polyacrylamide for the elimination of electroosmotic flow(20)and protein adsorption.

The coated capillary was rinsed with deionized water for 2 min and was then filled with a solution containing tau protein or model protein and 0.5% carrier ampholyte, Pharmalyte 3-10. Focusing was performed by applying a constant 500 V/cm electric field across the capillary for 15 min. The solutions of 20 mM phosphoric acid and 20 mM sodium hydroxide were used as the anolyte and the catholyte in the inlet and outlet reservoirs, respectively, which were kept at the same height during the focusing.

Once the focusing was complete, the focused protein zones were mobilized by combining gravity with cathodic mobilization. The electric potential was turned off and the outlet reservoir was removed. The capillary tip was fixed about 0.5 mm outside the electrospray needle. A sheath liquid composed of 50% acetone, 49% water, and 1% acetic acid (v/v/v) at pH 2.6 was delivered at a flow rate of 3 ml/min using a Harvard Apparatus 22 syringe pump (South Natick, MA). During the mobilization step, two HV power supplies were used for delivering the electric potentials of 20 and 5 kV to the inlet electrode and the electrospray needle, respectively. Detailed configuration of CIEF-ESIMS including sheath liquid and electrical connections was described elsewhere(8,9). To combine gravity with cathodic mobilizations, the inlet reservoir was raised 8 cm above the electrospray needle. No sheath gas was employed during the CIEF-ESIMS measurements. The first quadruple was scanned from m/z 750 to m/z 1400 at a scan rate of 1.2 sec/scan. The deconvoluted mass

spectra of protein analytes were obtained using the LC/MS BioToolBox analysis software from Perkin-Elmer (Foster City, CA).

Reversed-Phase LC/MS/MS Analysis of Phospho-tau Digestion Mixtures

All LC separations were performed using an Applied Biosystem (Fullerton, CA) 140A solvent delivery system at a flow rate of 40 ml/min. Peptide separations were carried out with a 1 mm i.d. x 25 cm Vydac reversed-phase C_{18} column (LC Packings, San Francisco, CA). Approximately 100 pmole of phosphorylated tau sample was injected for every LC/MS/MS LC/MS analysis. Solvent A was 0.1% TFA in water; solvent B was 0.1% TFA in acetonitrile/water (90:10, v/v). Separation of the tryptic peptides was effected with a gradient of 5% to 50% B in 50 min. Eluent from the LC column was directed to the mass spectrometer via a 15-cm-long fused-silica tubing with 50 mm i.d. and 192 mm o.d. (Polymicro Technologies, Phoenix, AZ).

The mass spectrometer used in this study also was the Finnigan MAT TSQ 700 (San Jose, CA) triple quadrupole equipped with an electrospray ionization source. LC-ESI MS of tryptic digests spectra were acquired by scanning Q1 from m/z 160 to m/z 2000 at a scan rate of 2.8 sec/scan. For the LC-ESI neutral loss MS/MS, tuning and calibration of the mass spectrometer were established using an acetic acid solution (methanol/water/acetic acid, 50:49:1 v/v/v) containing a synthetic phosphopeptide which has the same sequence as a phospho-tau tryptic fragment (*VAVVRTpPPKSPSSAK*). The neutral loss value monitored

was m/z 49. Q1 was set to scan m/z 160 to 1400 at a scan rate of 2 sec/scan and Q3 scanned

m/z from 111 to 1351. Argon collision gas was fed into Q2 with gas pressure of 1.6 mTorr

which was optimized for maximum precursor-ion intensity. The potentials at the heated

capillary, tube lens, and Q2 were set to be 26 V, 86 V, and -35 V, respectively. Detailed

conditions of neutral loss tandem MS were described and discussed elsewhere(17).

RESULTS AND DISCUSSION

CIEF-ESI MS for Tau Protein and Phosphorylation Analysis

At protein level, tau protein and its phosphorylation are studied using CIEF-ESI MS.

To investigate the electrospray ionization efficiency and the pI of recombinant tau, sample

was analyzed and characterized by CIEF-ESI-MS. Fig. 1A shows an electropherogram with

the deconvoluted molecular mass of native tau (peak 1) as 45760.0. The protein was

characterized on the basis of its mass spectrum which was taken from the average scans under

peak 1 of Fig. 1A (Fig. 1B). The high content of basic residues in tau leads to the highly

positively charged tau protein ions during the electrospray ionization at pH 2.6 in sheath

liquid. The envelope of tau ions was obtained from the average scan with m/z range from 700

to 1100. The pharmalyte ions similar to simple electrolyte ions led to high solution

conductivity and contributed to the establishment of the charge excess known to exist in

droplets formed during the electrospray process. Considering the effect of pharmalyte

concentration on the CIEF separation and the protein electrospray ionization mass spectra(8), a solution containing 0.5% pharmalyte 3-10 and tau or protein mixture was used in the CIEF-ESIMS measurements. Although most of the pharmalyte ion interference which occurs most at lower m/z values has been eliminated by acquiring the ion signals from m/z 700 to 1600, a broad band has been formed at a pI around 7-5.5 from pharmalyte 3-10 mixtures, as shown in Fig. 1A (peak 2). This result has been proved by running the CIEF-ESI-MS with only pharmalyte inside the capillary. For different ranges or brands of pharmalytes, the interference appeared at different pI ranges.

Tau's pI was determined with model proteins as internal standards in CIEF-ESI-MS analysis. Fig. 2A shows the reconstructed ion electropherogram of 0.1 mg/mL each of cytochrome C (pI 9.6), myoglobin I (pI 7.2), myoglobin II (pI 6.8), carbonic anhydrase I (pI 6.0), and recombinant tau protein. A good linear relationship was obtained (Fig. 2B) between migration time and pI values with the linear coefficient of 0.994. Tau's pI was determined as 8.0, which agreed fairly well with the result from IEF (pI=8.0).

Fig. 3A shows a reconstructed ion electropherogram of phospho-tau at 0.2mg/mL. The pI decreases at higher degrees of phosphorylation (peak 2) for the same protein, while the migration time increases with decreasing pI value. A continues increase in MW is observed along the broad peak which indicates that phosphorylation by PKA results in a heterogeneous phospho-tau mixture. The pI difference between two adjacent phospho-forms is too small to be resolved by CIEF. The pI of peak 2 in Fig. 3A is determined to be 7.5 by

using the same calibration method discussed above. The mass spectrum of tri-phosphotau

taken from the average scans under the peak is shown in Fig. 3B.

Model Peptide Analysis Using LC-ESI MS and LC-ESI Neutral-Loss MS/MS

To obtain good detection sensitivity, neutral loss monitoring was set up at m/z 49 for

the doubly or multiply charged peptide ions which are more abundant generated by ESI than

molecular peptide ions. The molecular weight of phosphoric acid is 98 and it should be the

product of neutral loss from the molecular phosphopeptide ions. The apparent neutral loss

is then $m98/n$ (where m = number of phosphoric acid loss and n = number of charges). This

equation can be used to determine the charge state (n) of detected ions. This is a more

complete equation than the one used before(19), where neutral loss = **98/n**, which neglected

the possibility of other multiple charged (n>2) peptides with more than one phosphate group

lost in neutral-loss MS/MS detection. To evaluate the on-line capability and sensitivity of

this LC-ESI MS and LC-ESI neutral-loss MS/MS technique, a 100 pmol total mixture of four

synthetic tau peptides was analyzed. Their sequences and molecular weights are shown in

Table I. The resulting RICs from LC-ESI MS and LC-ESI neutral-loss MS/MS are shown in

Fig. 4 A and B, respectively. As indicated by the good quality of these chromatograms, nice

intensity was obtained for both Q1 and neutral loss scanning. Positive confirmation of each

of the peptide peaks was obtained by evaluating their spectra (Fig. 5 A-D and Fig. 6 A-B).

For the LC-ESI MS spectra taken from the average scan under RIC peaks in Fig. 4A, the peptides were clearly identifiable by a series of multiply charged ions and their deconvoluted molecular masses as shown in Fig. 5 A-D. For the LC-ESI neutral-loss MS/MS spectra(Fig. 6 A-B), only one charged ion was detected for each peak, which is the doubly charged ion for both peptides. Considering $m98/n$ = 49, we should see doubly charged ions (n=2) from monophosphopeptides (m=1) when monitoring at m/z 49. Both phosphopeptides were detected and have very strong signals at 100 pmol. Their retention time were reproducible. These two peptides were phosphorylated at either serine or threonine and were able to release phosphoric acid through b-elimination. We have also tested a phosphopeptide at tyrosine, and were not able to see any signal in neutral loss MS/MS at 49(data not shown). It requires the cleavage of a bond to the stable aromatic ring for the loss of phosphoric acid and it is unlikely to happen under the neutral loss MS/MS condition. A b-elimination mechanism seen with serine or threonine is not possible with tyrosine.

Sensitivity of LC-ESI neutral-loss MS/MS was evaluated by analysis of successive dilutions of the 100 pmol total model peptide mixture. The final dilution results in 2 pmol of injection on LC column and its RIC is shown in Fig. 4C. Slight differences in retention time in RIC may be attributed to the decreased injection amount. Further dilution resulted in an indiscernible RIC, while the doubly charged ion spectra were still obtained around 750 fmol injection amount.

Characterization Tryptic Digests of Phospho-tau by PKA Using LC-ESI MS and LC-ESI Neutral-Loss MS/MS

The mass spectrometer is well toned for MS/MS neutral loss detection of phosphopeptides. We chose the scan range from m/z 160 to m/z 1400 mainly because of the high background noise beyond m/z1400. Good S/N for RIC and strong ion intensity were obtained for this setting. Informative RIC of ESI neutral loss MS/MS is obtained for the detection of phophopeptide in tryptic digests. Fig. 7B shows the RIC which exhibits 6 peaks which undergo loss of a neutral of m/z 49. All the peaks were identified based on their spectra. The spectra taken from the average scan under each peak from Fig. 7B are shown in Fig. 8 (A to F). Table II summarizes the identification of phosphopeptide ions detected by LC-ESI neutral-loss MS/MS from tryptic digests of PKA phospho-tau according to the following discussion.

Peak 1 in Fig. 7B gives a signal at m/z 802.2 (Fig. 8A). This value is very close to the theoretical m/z for the doubly charged monophosphoform of both tryptic peptides VAVVR/TPPK/SPSSAK (226-240) (m/z 802.4, z=2+) and IGSTENLKHQPGGGK (260-274) (m/z 801.9, z=2+). Although the detected m/z value is closer to the peptide (226-240), further information is needed to assign the peak and discussed later in this section.

Peak 6 in Fig. 7B has a m/z value of 653.4 (Fig. 8F) which is not close to any theoretical m/z value from the doubly charged tryptic peptides; However, it matches the theoretical m/z for the 4+ charged diphosphoforms of the tryptic peptide

SPSSAK/SR/LQTAPVPMPDLK/NVK (235-257) (m/z 653.6, z=4+). The size and hydrophobicity of the peptide also explain its late retention position.

The tryptic fragment SPSSAK, which is the only fragment with two phospho-sites in peak 6, also appears in VAVVR/TPPK/SPSSAK (226-240). So peak 1 is more likely to be the phosphoform of VAVVR/TPPK/SPSSAK since SPSSAK has been identified as being phosphorylated by PKA in peak 6. The most likely residue which can be phosphorylated on this sequence is Ser^{237}. It was reported that tau was phosphorylated by PKA exclusively on serine residues(21). The most favored site of phosphorylation in this tau tryptic peptide is the third N-terminal residue. The first residue is not known to be phosphorylated. In the case of the diphosphopeptide of this fragment, Ser^{237} and Ser^{238} are most likely to be the two phospho-sites. This view was further confirmed by total peptide mapping in LC-ESI MS. Phosphorylation of tau by PKA inhibits its proteolytic degradation(22) and may explain the fact that some of the tryptic phosphopeptides we detected contained undigested tryptic sites.

Peak 2 in Fig. 7B yielded two m/z signals of 695.0 and 750.8 (Fig. 8B). These values are consistent with the theoretical m/z for the doubly charged monophosphoforms of the tryptic peptides SR/TPSLPTPPTR (210-221) (m/z 695.3, z=2+) and TPSLPTPPTR/EPK (212-224) (m/z 750.9, z=2+), respectively. An ion with m/z 872.2 (Fig. 8C) was obtained from peak 3 in Fig 7B, and represents the doubly charged monophosphopeptide ion of SR/TPSLPTPPTR/EPK (210-224) (m/z 872.5, z=2+). All these three peptides are closely related to each other in terms of sequence and position in tau, and may explain the similarity

of their retention time. Their common tryptic fragment TPSLPTPPTR (212-221) enabled us to assign the phosphorylation site as Ser^{214}. This phospho-site for PKA has been reported by Scott(21).

Peak 4 in Fig. 7B gave a signal at m/z 893.6 (Fig. 8D) which is very close to the theoretical m/z for the doubly charged monophosphoform of IGSLDNITHVPGGGNK/K (354-370) (m/z 893.9, z=2+). The more intense signal obtained from peak 5 has a m/z value 829.1 (Fig. 8E) and represents the doubly charged monophosphopeptide ion of IGSLDNITHVPGGGNK (354-369) (m/z 829.9, z=+2). The phosphorylation site can be determined as Ser^{356} since there is only one serine in these two peptides. Again, the same site has been determined by Scott(21). Comparing the sequence of these two peptides, the hydrophobicity of above peptides would be expected to decrease if the C-terminal lysine is not cleaved by trypsin. This would give the longer peptide a shorter retention times.

The total peptide mapping (Fig 7A) from LC-ESI MS analysis provides some complementary information for the tryptic digest of phosphotau phosphorylated by PKA. The reproducible LC retention time makes it much easier to locate the phosphopetide peaks from the complicated LC-ESI MS profiles. It can be seen that all peaks from Fig 7B have the correlated peaks (Peak 1, 2, 3, 4, 5, 6). Since more than one ion was obtained for each peptide, more assurance can be given to the deconvoluted molecular weight based on the spectrum from total scanning than that from neutral loss scanning in which only one peptide can be detected. Thus LC-ESI MS is able to confirm the charge state of ions from neutral loss MS/MS. For example, the m/z 653.4 ion from peak 6 in Fig 7B has a z value of 4+, which

was further proved to be the diphospho-form of SPSSAK/SR/LQTAPVPMPDLK/NVK. Phosphorylation of VAVVR/TPPK/SPSSAK (226-240) is further confirmed by the appearance of peak 1^a in Fig. 7A. According to the deconvolution of this peak (MW=1682.9) and its retention which is very close to monophospho-VAVVR/TPPK/SPSSAK (MW=1602.9), the peak is likely to be the diphosphoform of VAVVR/TPPK/SPSSAK. Besides, no other tryptic peptide has the close MW value of 1682.9 The other possible peptide for peak 1 can be ruled out since there is no second serine in its sequence so its diphosphoform hardly exists. The correlating ion of this diphosphopeptide was not found in Fig 7B. The signal might be too weak to be detected by LC-ESI neutral-loss MS/MS.

Determination of Phosphorylation Percentage on Each Phospho-site by PKA from RIC of LC-ESI MS

The percentage of phosphorylation of each phospho-site was calculated based on the peak intensity from the deconvolution of spectra under the RIC peaks. The assumption that all the phospho- and dephospho- peptides correlating to the site are found enables an approximate determination of the phosphorylation percentage. Deconvoluted peak intensity instead of peak intensity of in RIC was utilized for calculation because of the fact that the deconvoluted peak intensity is proportional to a peptide concentration while the peak in RIC could include more than one peptide components.

The deconvoluted molecular peptide intensities with calculated phosphorylation percentage are listed in Table III. Row 1 shows all the possible peptides related to the phospho-sites Ser^{237} or Ser^{238}. Three phosphopeptides (VAVVR/TPPK/SPSpSAK, VAVVR/TPPK/SPSpSpAK and SPSpSpAK/SR/LQTAPVPMPDLK/NVK) with their intensities and peak numbers are compared with the only one dephosphopeptide located in Fig 6A as peak a (TPPK/SPSSAK). The phosphorylation percentage are 85.4% at Ser^{237} and 10.2% at Ser^{238}.

All the possible peptides related to the phospho-site Ser^{214} (SR/TPSpLPTPPTR, TPSpLPTPPTR/EPK, and SR/TPSpLPTPPTR/EPK) and their intensities are shown in row 2 of Table III. No correlating dephosphopeptide was found in Fig 7A. The results strongly suggested the phosphorylation at Ser^{214} is complete.

Table III row 3 give all the possible peptides related to the phospho-site of Ser^{356}. Two phosphopeptides (IGSpLDNITHVPGGGNK/K and IGSpLDNITHVPGGGNK), their intensities and peak numbers are listed. Two dephosphopeptides were identified in Fig 7A as peak b and c (IGSLDNITHVPGGGNK/K and IGSLDNITHVPGGGNK), respectively . The phosphorylation percentage is determined as 67.6% at Ser^{356}.

The observed phosphorylation stoichiometry for PKA is 2.63 mol p/mol tau. Compare to the experimental value 3.41 mol p/mol tau for PKA, analyzed by Cherenkov counting of ^{32}P-labeled tau, the stoichiometry value from our experiment is slightly low. Our determination can be accurate only if all phospho-sites are identified and all the correlating phospho- and dephospho- forms are found. This can not be guaranteed in our current

experiment. Since neutral loss MS/MS scanning range was from m/z 160 to 1400, it is

possible that some ions with high m/z value (larger than 2800 for monophospho-peptides)

are missing in our measurements. Nevertheless, the result agrees fairly well between the two

methods.

Characterization Tryptic Digests of Phospho-tau by MBR kinase from Rat Brain Using LC-ESI MS and LC-ESI Neutral-loss MS/MS

Fig. 9B shows the RIC of LC-ESI neutral-loss MS/MS from phospho-tau tryptic digest

by MBR kinase purified from rat brain. All 6 peaks (labeled as 1', 2', 3', 4', 5' and 6') are

identified as phosphopeptides based on their spectra. The spectra taken from the average

scan under each peak from Fig. 9B are shown in Fig. 10 (A to F). Table IV is a summary of

the identification of the phosphopeptide ions from tryptic digests of MBR kinase phospho-

tau detected by LC-ESI neutral-loss MS/MS.

Peak 1' in Fig. 9B gave a signal at m/z 801.6 (Fig. 10A). Again, this m/z is very close to

both theoretical values of the doubly charged monophosphopeptides

VAVVR/TPPK/SPSSAK (226-240) (m/z 802.4) and IGSTENLK/HQPGGGK (260-274)

(m/z 801.9). Notice that the retention time of this peak differs from that of peak 1 in Fig. 7

assigned as the monophosphoform of VAVVR/TPPK/SPSSAK (see discussion above). The

peptide in peak 1' was determined as IGSpTENLK/HQPGGGK (260-274) further in aid

with the assignments of peak 2' and peak 3' in Fig. 9B. Peak 2' has a m/z value of 578.7

(Fig. 10B) and was determined without any ambiguity as the doubly charged ion of monophosphopeptide SK/IGSTENLK (258-267). This peptide has a retention very close to peak 1' and has a common sequence IGSTENLK as peak 1'. Note that the common sequence IGSTENLK from peak 1' and 2' has only one Ser^{262} which should be the phospho-site for both peptides.

The appearance of peak 3' in Fig. 9B with m/z of 802.2 (Fig. 10C) and with retention time same as Peak 1 in Fig. 7 is the monophosphoform of VAVVR/TPPK/SPSSAK (226-240). The phosphorylation site is Ser^{237} or Ser^{238}

One weak signal was detected as Peak 4' in Fig. 9B with m/z value of 872.2 (Fig. 10D) consistent with the theoretical m/z for the doubly charged monophospho-SR/TPSLPTPPTR/EPK (210-224) (m/z 872.5, z=2+). Having the same m/z and retention, peak 4' is identical to Fig. 7B peak 3 with the phosphorylation site at Ser^{214}.

Peak 5' in Fig. 9B gave a signal at m/z 893.6 (Fig. 10E) which is the doubly charged monophosphoform of IGSLDNITHVPGGGNK/K (354-370) (m/z 893.9, z=2+). Peak 6' with the m/z value 829.1 (Fig. 10F) represents the doubly charged monophosphopeptide ion of IGSLDNITHVPGGGNK (354-369) (m/z 829.9, z=2+). These two peaks correspond to the peak 4 and 5 in Fig. 7, respectively. The phosphorylation site is at Ser^{356}.

The total peptide mapping from LC ESI MS analysis is shown in Fig. 9A. All peaks from Fig. 9B have the correlated peaks (Peak 1', 2', 3', 4', 5', 6'). Additional information from Fig. 9A further confirms the phospho-site at Ser^{262}. The peak of $IGS^{262}TENLK$ (260-267), which was found in phospho-tau peptide map of PKA, disappeared in the map of

MBR kinase. The phospho-peptides may resist tryptic digestion and exist as longer forms as IGSpTENLK/HQPGGGK in peak 1' and SK/IGSpTENLK in peak 2'.

Determination of Phosphorylation Percentage on Each Phospho-site by MBR kinase from Rat Brain from RIC of LC-ESI MS

The phosphorylation percentage of each site phosphorylated by MBR kinase, as done for PKA phosphorylation, was calculated based on the peak intensity from the deconvolution of spectra under the RIC peaks.

The deconvoluted molecular peptide peaks are summarized in Table V. Row 1 shows all the possible peptides related to the phospho-site Ser^{262}. Two phosphopeptides (IGSpTENLK/HQPGGGK and SK/IGSpTENLK) and their intensities listed were deconvoluted from Fig. 9A peak 1' and 2', respectively. As no correlating dephosphopeptide was found in RIC, it may be concluded that phosphorylation at Ser^{262} is complete.

Row 2 shows all the possible peptides related to the phospho-sites Ser^{237} and/or Ser^{238}. Two phosphopeptides (VAVVR/TPPK/SPSpSAK and VAVVR/TPPK/SPSpSpAK) and their intensities were obtained with only the first one was detected by neutral loss MS/MS. One dephosphopeptide was located in Fig. 9A as peak a (TPPK/SPSSAK). The phosphorylation percentage are 3.26% at Ser^{237} and 1.41% at Ser^{238}.

Row 3 shows all the possible peptides related to the phospho-site of Ser^{214}. One weak peak of SR/TPSpLPTPPTR/EPK and its intensity is deconvoluted from Fig 12A peak 4'. Three dephospho-peptides coeluted in Fig 12A peak b' having sequences of SR/TPSLPTPPTR/EPK (210-224), SR/TPSLPTPPTR (210-221) and TPSLPTPPTR/EPK (212-224), respectively (Fig. 16B). The phosphorylation percentage is only 0.7% at Ser^{214}.

Row 4 gives all the possible peptides related to the phospho-site Ser^{356}. Two phosphopeptides (IGSpLDNITHVPGGGNK/K and IGSpLDNITHVPGGGNK) and their intensities are from Fig. 9A peak 5' and 6', respectively. Two dephosphopeptides were located in Fig. 9A as peak c' and d' (IGSLDNITHVPGGGNK/K and IGSLDNITHVPGGGNK). The phosphorylation percentage is determined as 63.5% at Ser^{356}.

The two major phospho-sites of this kinase are Ser^{262} and Ser^{356} which are both of in the microtubule binding domain of tau protein. The observed phosphorylation stoichiometry for this kinase is 1.69 mol p/mol tau. Compare to the experimental value analyzed by Cherenkov counting of ^{32}P-labeled tau which was 1.70 mol p/mol tau for this kinase, the agreement is quite well. As we discussed before, the determination based on the peak intensity can only be accurate when all phospho-sites are identified and all the correlating phospho- and dephospho - forms are found. Phosphopeptide ions from phospho-tau of MBR kinase are presented mainly in the low m/z value within the scanning range of m/z 160 to 1400, therefore no significant amount ions were lost in neutral loss MS/MS.

CONCLUSION

By using CIEF-ESI-MS, we successfully determined the pI of recombinant tau protein and characterized phospho-tau at the intact protein level. Using a model phospho- and dephospho- peptide mixture, the condition of LC-ESI neutral loss MS/MS was improved and optimized for phosphopeptide detection. On-line RP-HPLC-ESI-MS and RP-HPLC-ESI neutral loss MS/MS were effectively combined for the determination of phosphorylation locations, and was successfully applied to the tryptic digest of tau proteins phosphorylated by two different kinases. For PKA, the main phospho-sites (21), Ser^{214} and Ser^{356} were identified and some additional phospho-sites, Ser^{237} and Ser^{238}, were discovered the first time. For MBR kinase purified from rat brain, the two major phospho-sites in microtubule binding domain, Ser^{262} and Ser^{356} and some other minor phospho-sites were found in this new improved analysis. The phosphorylation stoichiometry was also evaluated based on peptide intensities deconvoluted from RIC of LC-ESI MS; However, the requirement for the accuracy of this determination is rather critical. These approaches are highly promising for further characterization of phosphorylation reactions and might be used for the diagnosis at normal phosphorylation event in Alzheimer's disease.

ACKNOWLEDGMENT

REFERENCES

1. Hubbard, M. J., and Cohen, P. (1993) *Trens. Biochem. Sci.* **18**, 172-177

2. Schweers, O., Schonbrunn-Hanebeck, E., Marx, A., and Mandelkow, E. (1994) *J. Biol. Chem.* **269**, 24290-24297

3. Goedert, M., Spillantini, M. G., Jacks, R., Ruthord, D., and Crowther, R. A. (1989) *Neuron* **3**, 519-526

4. Greenberg, S. G., Davies, P., Schein, J. D., and Binder, L. I. (1992) **267**, 564-569

5. Goedert, M., Spillantini, M. G., Cairns, N. J., and Crowther, R. A. (1992) *Neuron* **8**, 159-168

6. Lee, V. M.-Y., Olvos, B. J., and Trojanowski, J. O. (1991) *Science* **251**, 675-678

7. Harrison, J. C. (1992) in *Protein Phosphorylation - A Pratical Research* (Hardie, D. G., ed), pp. 22, Oxford University Press, New York

8. Tang, Q., Harrata, A. K., and Lee, C. S. (1995) *Anal. Chem.* **67**, 3515-3519

9. Tang, Q., Harrata, A. K., and Lee, C. S. (1996) *Anal. Chem.* **68**, 2482-2487

10. Tang, Q., Harrata, A. K., and Lee, C. S. (1997) *Anal. Chem.* **69**, 3177-3182

11.   Yang, L., Tang, Q., Harrata, A. K., and Lee, C. S. (1996) *Anal. Biochem.* **243**, 140-149

12.   Yip, T. T., and Hutchens, T. W. (1992) *FEBS letts* **308**, 149-153

13.   Liao, P. C., Leykam, J., Andrews, P. C., Gage, D. A., and Allision, J. (1994) *Anal. Biochem.* **219**, 9-20

14.   Craig, A. G., Hoeger, C. A., Miller, C. L., Goedken, T., and River, J. E. (1994) *Biol. Mass Spectrom.* **23**, 519-528

15.   Annan, R. S., and Carr, S. A. (1996) *Anal. Chem.* **68**, 3413-3421

16.   Gibson, B. W., and Gohen, P. (1990) *Methods Enzymol* **193**, 480

17.   Hunter, A. P., and Games, D. E. (1994) *Rapid Communications in Mass Spectrometry* **8**, 559-570

18.   Covey, T., Sushan, B., Bonner, R., Schroder, W., and Hucho, F. (1991) in *Methods in Protein Sequence Analysis* (Jornvall, H., Hoog, J. O., and Gustavsson, A. M., eds), pp. 249, Birkhauser Verlag, Basel

19.   Kebarle, P., and Tang, L. (1993) *Anal. Chem.* **65**, 972A

20.   Kilar, F., and Hjerten, S. (1989) *Electrophoresis* **10**, 23-29

21.   Scott, C. W., Spreen, R. C., Herman, J. L., Chow, F. P., Davison, M. D., Young, J., and Caputo, C. B. (1993) *The Journal of Biological Chemistry* **268**(2), 1166-1173

22.   Litersky, J. M., and Johnson, G. V. W. (1992) *J. Biol. Chem.* **259**, 5301-5305

Figure Legends

Fig. 1   A. CIEF-ESIMS reconstructed total ion electropherogram of tau protein at

concentration of 0.1 mg/mL. Capillary, 25 cm total length, 50 mm i.d. and 192 mm

o.d.; voltages, 15 kV for focusing and mobilization, 5 kV for electrospray; sheath

liquid, methanol/water/acetic acid (50:49:1, v/v/v) at pH 2.6, 3 ml/min; mass scan,

m/z 800 to 1100 at 1.2 sec/scan. B. Positive electrospray ionization mass spectrum

of tau protein taken from the average scans under the peaks in A. The inset of A

presents the deconvoluted molecular mass of tau.

Fig. 2   A. CIEF-ESIMS reconstructed total ion electropherogram of tau protein and model

proteins at concentration of 0.1 mg/mL for each component. Other conditions are

same as in Figure 2A. From peak 1 to peak 5 are cytochrome c, tau, myoglobin I,

myoglobin II, and carbonic anhydrase I. B. Plot of retention time vs. pI.

Fig. 3   A. CIEF-ESIMS reconstructed total ion electropherogram of

phosphorylated tau protein at concentration of 0.2 mg/mL. Other conditions are

same as in Figure 1A. The di- and tri-phosphotau variants are indicated and marked

as 1 and 2, respectively. Peak 3 is from parmalyte 3-10. B. Positive electrospray

ionization mass spectrum of tau protein taken from the average scans under the

peak 2 in A. The insert of A presents the deconvoluted molecular mass of

phosphorylated tau.

Fig. 4   LC-ESI MS (A) and LC-ESI neutral loss MS/MS (B) analysis of total 100 pmol

model peptide mixture. LC-ESI neutral loss MS/MS analysis of the 2 pmol model

peptide mixture.

Fig. 5   Positive electrospray ionization mass spectra from the LC-ESI MS analysis at total

100 pmol peptide level shown in Fig. 4A. Spectra of (A), (B), (C), and (D) are

taken from the average scans under the peak of P1', P1, P2' and P2, respectively.

The inserts present the deconvoluted molecular mass of each peptide.

Fig. 6   Positive electrospray ionization mass spectra from the LC-ESI neutral loss MS/MS

analysis at total 100 pmol peptide level shown in Fig. 4B. Spectra of (A) and (B)

are taken from the average scans under the peak of P1' and P2', respectively. The

obtained ions are doubly charged ions.

Fig. 7   LC-ESI MS (A) and LC-ESI neutral loss MS/MS (B) reconstructed ion

chromatogram (RIC) of PKA phosphotau tryptic digest. The correlated peak

number represents the same peptide component. The peak labeled with a letter is

dephosphorylated peptide with a possible phospho-site.

Fig. 8   Positive electrospray ionization mass spectra from the LC-ESI neutral loss MS/MS

of PKA phosphotau tryptic digest analysis shown in Fig. 7B. Spectra of (A), (B),

(C), (D), (E), and (F) are taken from the average scans under the peak with the peak

number of 1, 2, 3, 4, 5, 6, respectively.

Fig. 9   LC-ESI MS (A) and LC-ESI neutral loss MS/MS (B) RIC of MBR kinase

phosphotau tryptic digest.   The correlated peak number represents the same

peptide component.

Fig. 10   Positive electrospray ionization mass spectra from the LC-ESI neutral loss MS/MS

of MBR kinase phosphotau tryptic digest analysis shown in Fig. 9B. Spectra of

(A), (B), (C), (D), (E), and (F) are taken from the average scans under the peak with

the peak number of 1', 2', 3', 4', 5', 6', respectively.

TABLE I

Synthetic Tau Peptides

Peptides	Sequences	Molecular Weight (dalton)
P1	KSKIGSTENLK (257-267)	1203.0
P1'	KSKIGS*p*TENLK (257-267)	1283.0
P2	VAVVRTPPKSPSSAK (226-240)	1522.9
P2'	VAVVRT*p*PPKSPSSAK (226-240)	1602.9

TABLE II

Phosphopeptide Ions from PKA Phospho-tau Tryptic Digest Detected by LC-ESI Neutral Loss MS/MS at m/z 49

Peak number	z	m/z Observed	m/z Theoretical	Predicted peptide[a]	Phosphorylation site
1	2+	802.2	802.4	K<VAVVR/TPPK/S^{b}PS^{b}S^{b}AK>S (226-240)	Ser^{235}, Ser^{237}or Ser^{238}
6	4+	653.4	653.6	K<S^{c}PS^{c}S^{c}AK/SR/LQTAPVPMPDLK/NVK>S (235-257)	Ser^{235}, Ser^{237}or Ser^{238}
2	2+	695.0	695.3	R<SR/TPSpLPTPPTR>E (210-221)	Ser^{214}
2	2+	750.8	750.9	R<TPSpLPTPPTR/EPK>K (212-224)	Ser^{214}
3	2+	872.2	872.5	R<SR/TPSpLPTPPTR/EPK>K (210-224)	Ser^{214}
4	2+	893.6	893.9	K<IGSpLDNITHVPGGGNK/K>I (354-370)	Ser^{356}
5	2+	829.1	829.9	K<IGSpLDNITHVPGGGNK>K (354-369)	Ser^{356}

a. Numbers in parentheses represent the location of the peptide in the primary sequence of recombinant tau.
b. One of these three serines is phosphorylated.
c. Two of these three serines are phosphorylated.

TABLE III

Percentage of Phosphorylation by PKA based on the Peptide Intensity Deconvoluted from

LC-ESI MS Reconstructed Ion Chromatogram

Phosphorylation site		Detected peptides	Peak #	MW	Ion intensity	Phosphorylation percentage
Ser[237], Ser[238]	phospho-	K<VAVVR/TPPK/S^{b}PS^{b}S^{b}AK>S (226-240)	1^a	1682.9	1.0x10^7	85.4 %
		K<VAVVR/TPPK/S^{a}PS^{a}S^{a}AK>S (226-240)	1	1602.9	3.1x10^8	10.2%
		K<S^{b}PS^{b}S^{b}AK/SR/LQTAPVPMPDLK/NVK>S (235-257)	6	2610.6	3.2x10^7	
	dephospho-	K<TPPK/SPSSAK>S (231-240)	a	999.0	6.0X 10^7	
Ser[214]	phospho-	R<TPSpLPTPPTR>E (210-221)	2	1388.7	5.1x10^8	100.0%
		R<TPSpLPTPPTR/EPK>K (212-224)	2	1499.9	2.0x10^8	
		R<SR/TPSpLPTPPTR/EPK>K (210-224)	3	1743.0	6.0x10^7	
	dephospho-	none				
Ser[356]	phospho-	K<IGSpLDNITHVPGGGNK/K>I (354-370)	4	1786.0	2.8X10^7	67.6%
		K<IGSpLDNITHVPGGGNK>K (354-369)	5	1658.0	2.0X10^8	
	dephospho-	K<IGSLDNITHVPGGGNK/K>I (354-370)	b	1706.0	9.5x10^6	
		K<IGSLDNITHVPGGGNK>K (354-369)	c	1577.0	1.0x10^8	

a. One of these three Serines is phosphorylated.
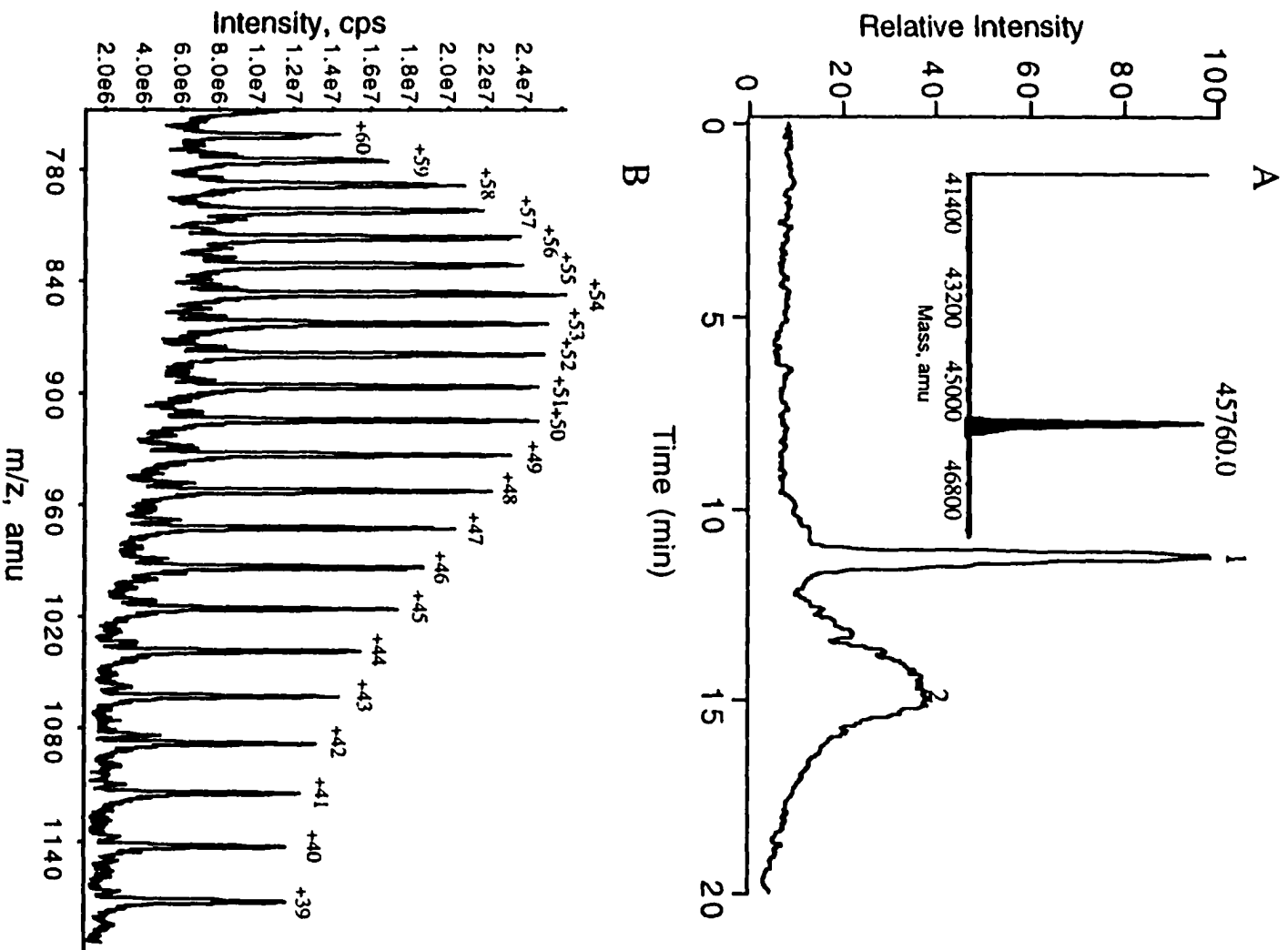b. Two of these three Serines are phosphorylated.

92

TABLE IV

Phosphopeptide Ions from MBR Kinase Phospho-tau Tryptic Digest Detected by LC-ESI Neutral Loss MS/MS at m/z 49

Peak number	z	m/z		Predicted peptide[a]	Phosphorylation site
		Observed	Theoretical		
1'	2+	801.6	801.9	K<IGSpTENLK/HQPGGGK>V (260-274)	Ser^{262}
2'	2+	578.6	578.8	K<SK/IGSpTENLK>H (258-267)	Ser^{262}
3'	2+	802.2	802.4	K<VAVVR/TPPK/S^{b}PS^{b}S^{b}AK>S (226-240)	Ser^{235}, Ser^{237}or Ser^{238}
4'	2+	872.2	872.5	R<SR/TPSpLPTPPTR/EPK>K (210-224)	Ser^{214}
5'	2+	893.6	893.9	K<IGSpLDNITHVPGGGNK/K>I (354-370)	Ser^{356}
6'	2+	829.1	829.9	K<IGSpLDNITHVPGGGNK>K (354-369)	Ser^{356}

a. Numbers in parentheses represent the location of the peptide in the primary sequence of recombinant tau.

b. One of these three Ser is phosphorylated.

TABLE V

Percentage of Phosphorylation by MBR Kinase Based on the Peptide Intensity Deconvoluted from

LC-ESI MS Reconstructed Ion Chromatogram

Phosphorylation site		Detected peptides	Peak #	MW	Ion intensity	phosphorylation percentage
Ser^{262}	phospho-	K<IGSpTENLK/HQPGGGK>V (260-274)	1'	1602.0	3.3x10^8	100.0%
		K<SK/IGSpTENLK>H (258-267)	2'	1155.0	5.3x10^8	
	dephospho-	none				
Ser^{235}, Ser^{237}, Ser^{238}	phospho-	K<VAVVR/TPPK/S^{a}PS^{a}S^{a}AK>S (226-240)	3'	1682.9	4.6x10^6	3.62%
		K<VAVVR/TPPK/S^{b}PS^{b}S^{b}AK>S (226-240)	3'	1602.9	5.5x10^6	1.41%
	dephospho-	K<TPPK/SPSSAK>S (231-240)	a'	999.0	3.0x10^8	
Ser^{214}	phospho-	R<SR/TPSpLPTPPTR/EPK>K (210-224)	4'	1743.0	9.0x10^6	0.7%
	dephospho-	R<SR/TPSLPTPPTR/EPK>K (210-224)	b'	1623.0	6.4x10^8	
		R<SR/TPSLPTPPTR>E (210-221)	b'	1309.0	4.6x10^8	
		R<TPSLPTPPTR/EPK>K (212-224)	b'	1420.0	6.7x10^7	
Ser^{356}	phospho-	K<IGSpLDNITHVPGGGNK/K>I (354-370)	5'	1786.0	5.6X10^7	63.5%
		K<IGSpLDNITHVPGGGNK>K (354-369)	6'	1658.0	4.0X10^8	
	dephospho-	K<IGSLDNITHVPGGGNK/K>I (354-370)	c'	1706.0	2.0x10^7	
		K<IGSLDNITHVPGGGNK>I (354-369)	d'	1578.0	2.6x10^8	

a. One of these three Serines is phosphorylated.
b. Two of these three Serines are phosphorylated.

Figure 1

Figure 2

A

43400 44800 46200 47600
Mass, amu

45920.0

43400 44800 46200 47600
Mass, amu

46000.9

Relative Ion Intensity

0   20   40   60   80   100

Time (min)

0   5   10   15   20

B

Intensity, cps

3.0e6   4.0e6   5.0e6   6.0e6   7.0e6   8.0e6   9.0e6

m/z, amu

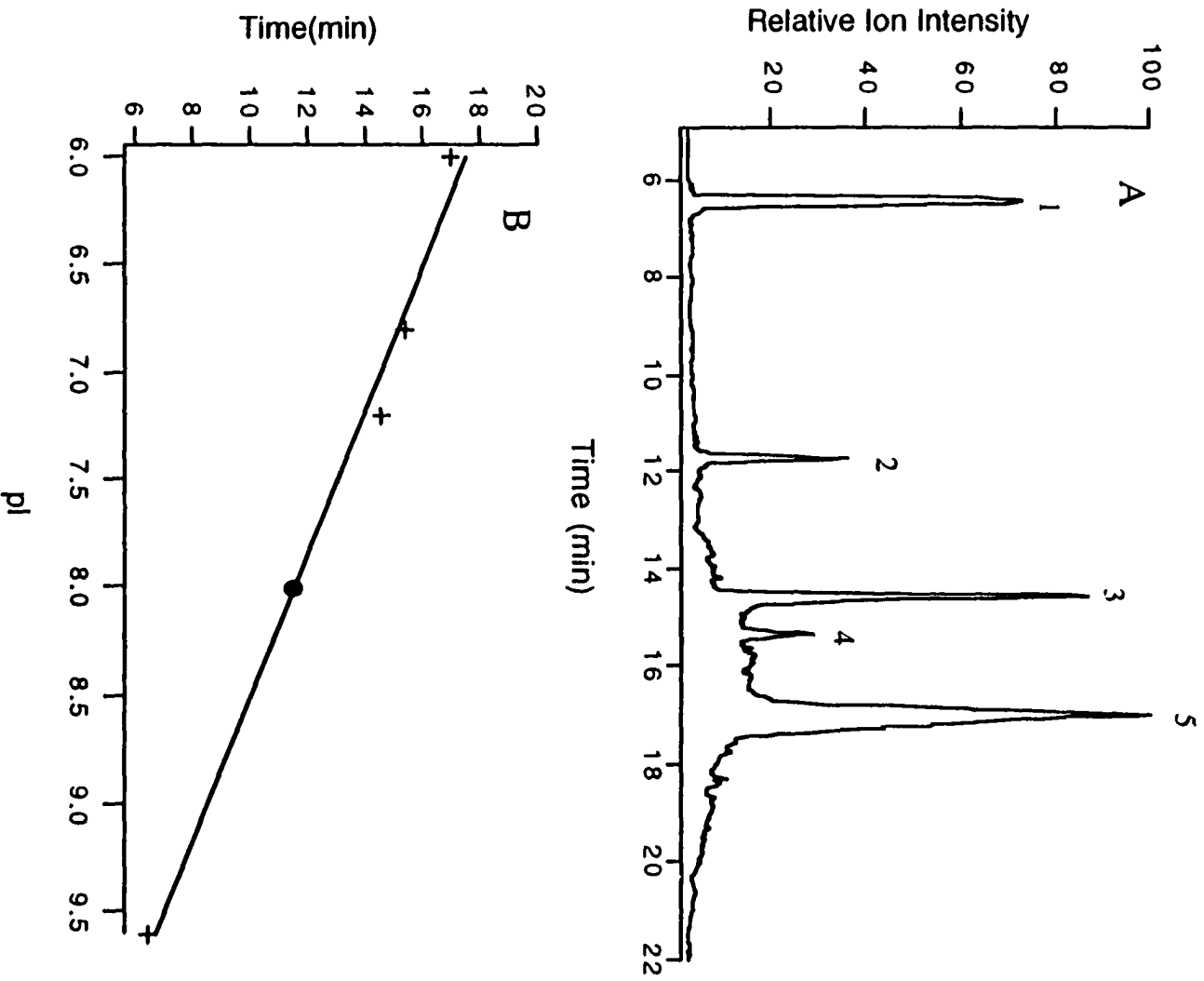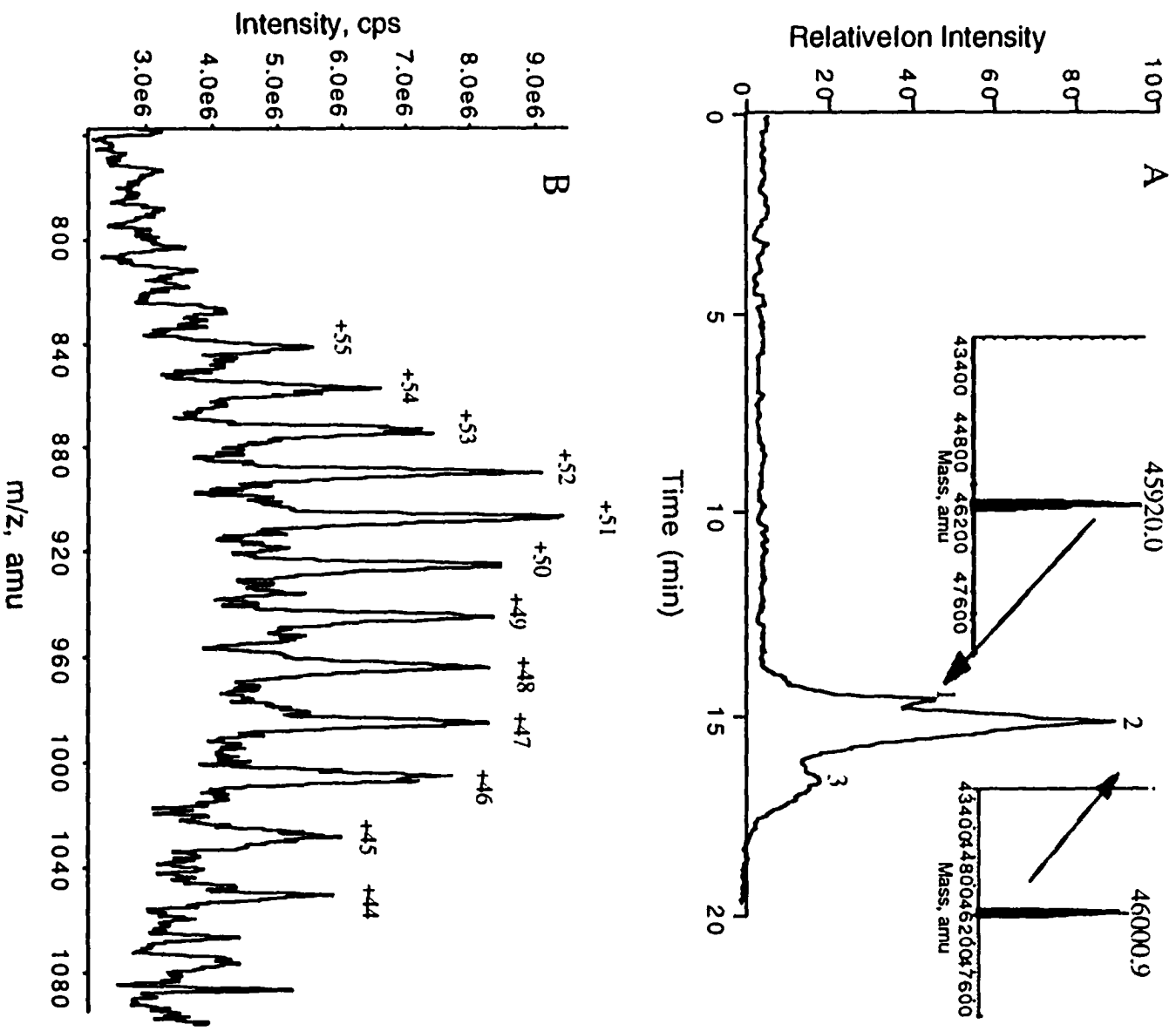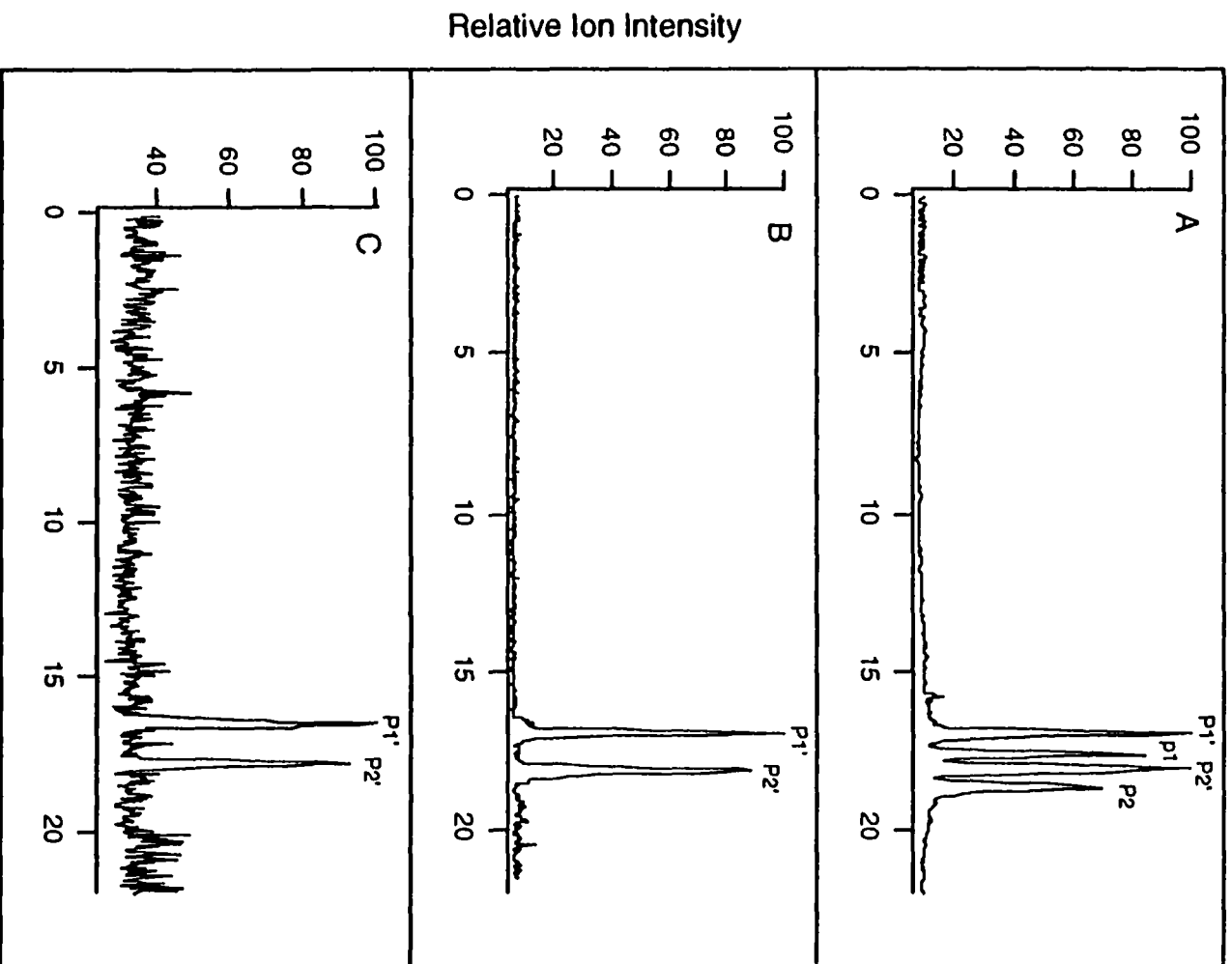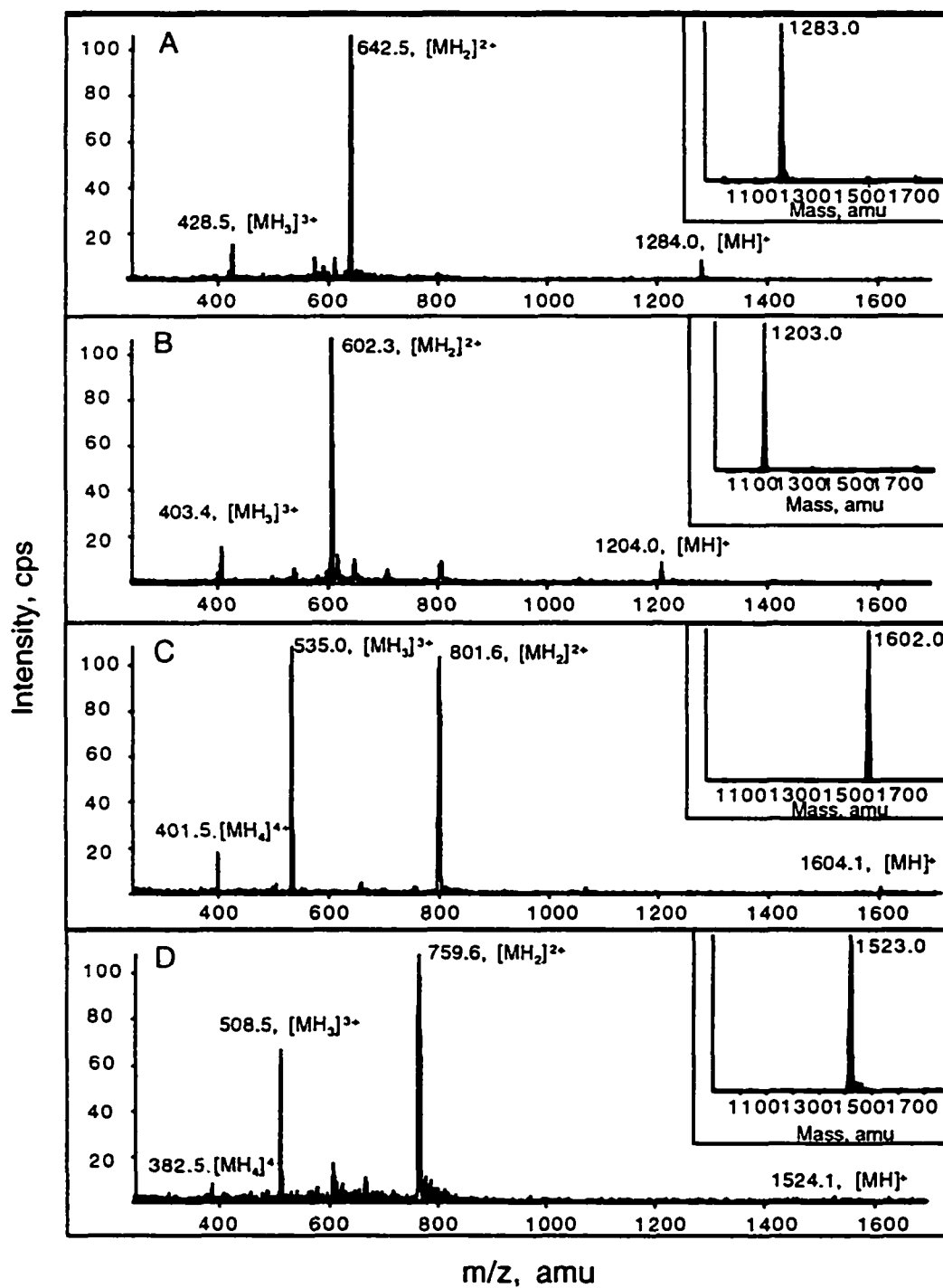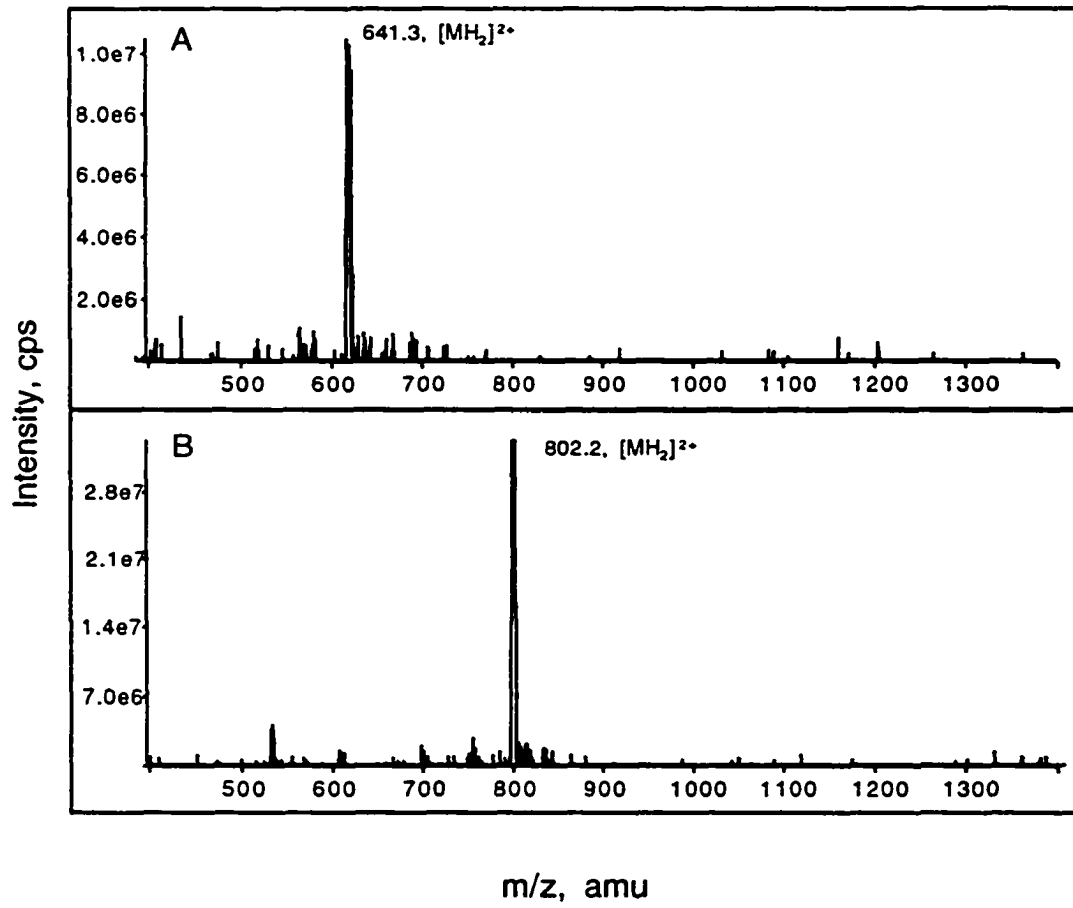800   840   880   920   960   1000   1040   1080

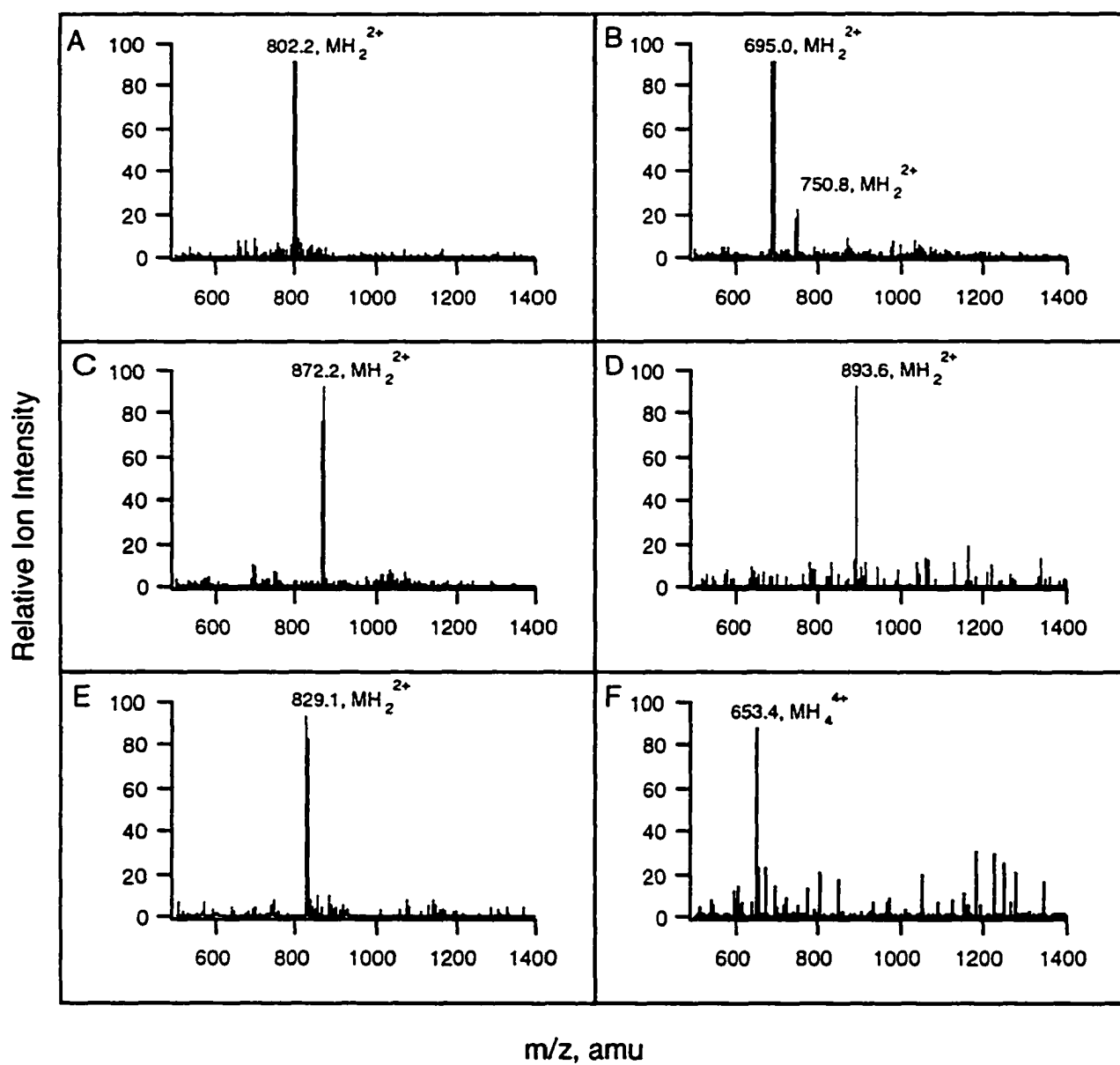+44 +45 +46 +47 +48 +49 +50 +51 +52 +53 +54 +55

Figure 3

Figure 4

Figure 5

Figure 6

Figure 7

101
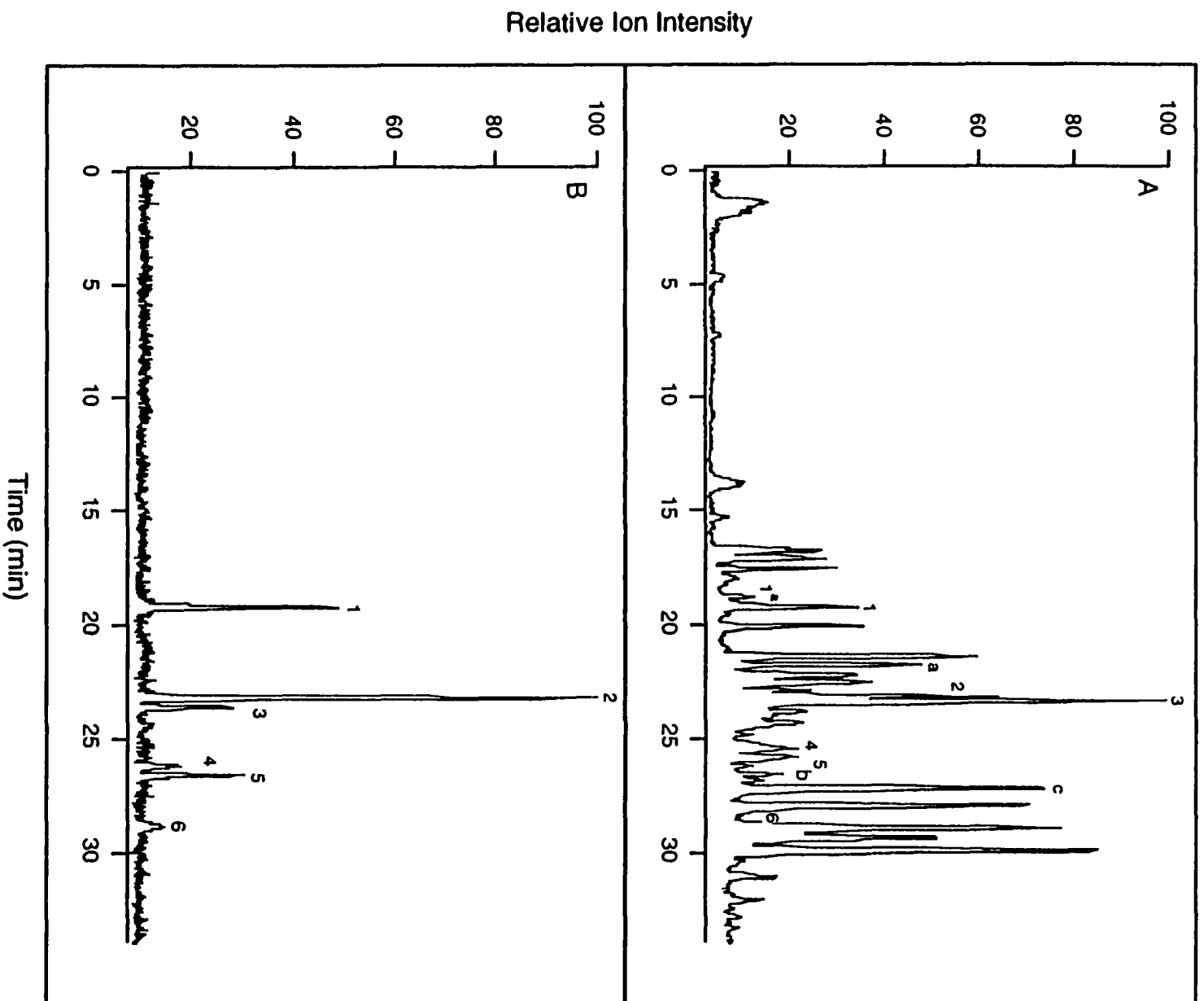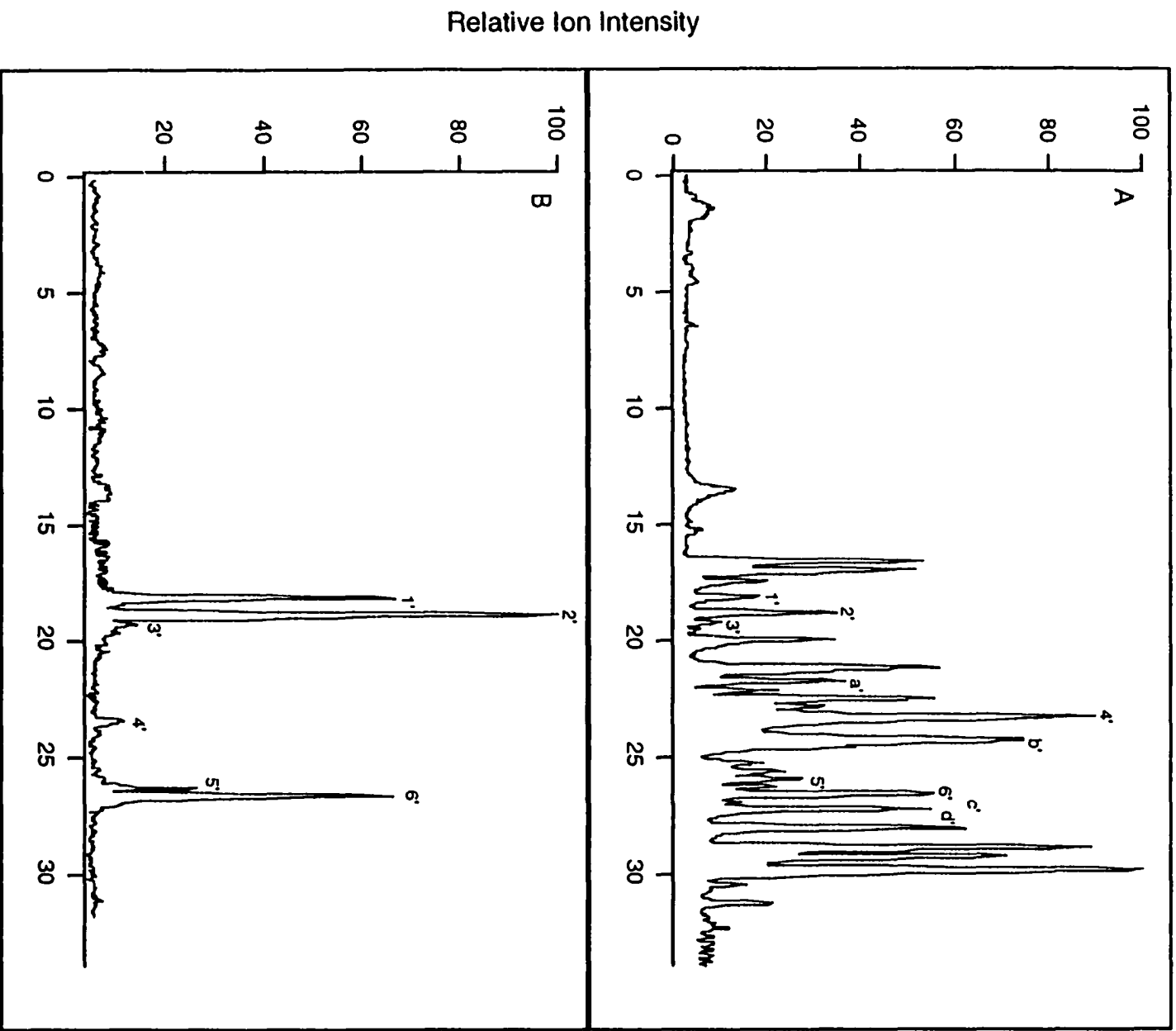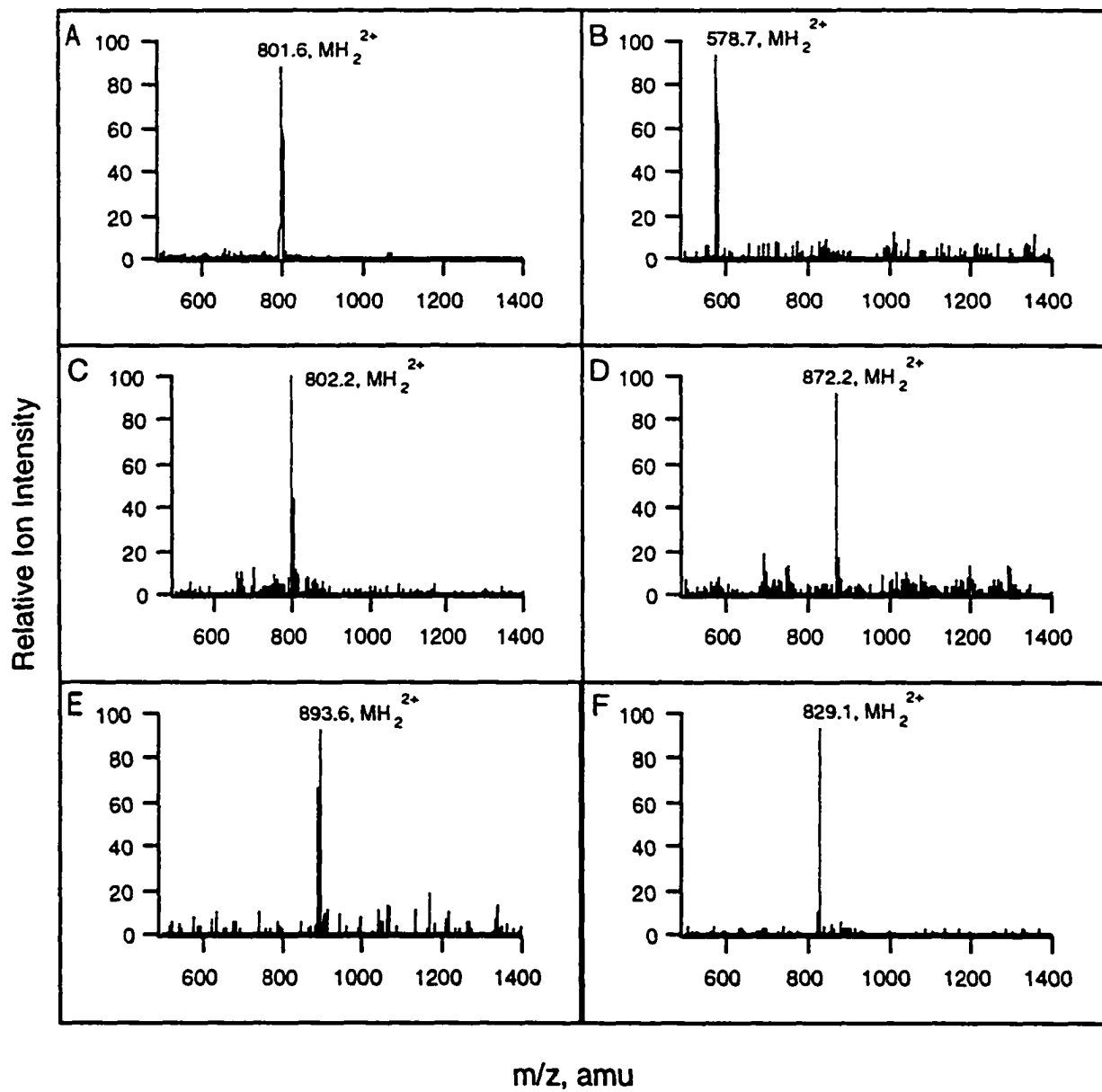
Figure 8

Figure 9

Figure 10

GENERAL SUMMARY

Methods have been developed to characterize protein/peptide phosphorylation using electrophoretic or chromatographic separation techniques coupling with mass spectrometers. On-line capillary isoelectric focusing (CIEF)-electrospray ionization mass spectrometry (ESIMS) is utilized for phosphorylation characterization at the intact protein level. Advantages of this technique for phosphorylation analysis are addressed by obtaining the two dimensional information: isoelectirc point and molecular weight.

At the peptide level, on-line RP-HPLC-ESI-MS and RP-HPLC-ESI neutral loss MS/MS were highly specific for the determination of phosphorylation locations, which was successfully applied on the tryptic digest of tau proteins phosphorylated by different kinases. Issues such as detection limit, sensitivity and conditions of mass spectrometer are addressed. The phosphorylation stoichiometry was also evaluated based on peptide intensities. These approaches are highly promising for further tau phosphorylation characterization and might be used for pursuing the diagnosis and treatment of Alzheimer's Disease .

On-line combination of CIEF with ESI-TOF MS is demonstrated for high resolution analysis of some model proteins and human hemoglobin variants. The successful coupling of these two techniques allows the optimization the efficiency of CIEF separation since TOF MS is the detector to produce a full spectrum in the shortest response time among all kinds

of mass analyzers. An efficient design interface device is needed to minimize the time loss

between focusing and mobilizing steps of CIEF in this technique.

REFERENCES

1. J. W. Jorgenson, and K. D. Lukacs, *Anal. Chem.*, **53**, (1981) 1298.

2. J. W. Jorgenson, and K. D. Lukacs, *J. Chromatogr.*, **218**, (1981) 209.

3. S. Hjerten, and M. D. Zhu, *J. Chromatogr.*, **327**, (1985) 157.

4. S. Hjerten, *J. Chromatogr.*, **270**, (1983) 1.

5. A. S. Cohen, A. Paulus, and B. L. Karger, *Chromatographia*, **24**, (1987) 15.

6. B. L. Karger, A. S. Cohen, and A. Guttman, *J. Chromatogr.*, **492**, (1989) 585.

7. P. Bocek, M. Deml, P. Gebauer, and V. Dolnik, *Anal. Isotachophoresis*, VCH Verlagsgesellschaft, Weinhein, (1988)

8. F. M. Everaerts, and P. E. M. Verheggen, in *New Directions in Electrophoretic Methods* (Jorgenson, J. W., and Phillips, M., eds), Vol. 335, Amer. Chem. Soc. Symp., Washington D. C., 1987, Chap. 4.

9. J. H. Knox, *Chromatographia*, **26**, (1988) 329.

10. J. R. Mazzeo, and I. S. Krull, *Bio Techniques*, **10**, (1991) 638.

11. S. Hjerten, *J. Chromatogr*, **347**, (1985) 191.

12. S. Hjerten, K. Elenbring, F. Kilar, J. L. Liao, J. C. Chen, C. J. Siebert, and M. D. Zhu, *J. Chromatogr.*, **403**, (1987) 47.

13. S. Hjerten, J. Liao, and K. Yao, *J. Chromatogr.*, **387**, (1987) 127.

14. S. Hjerten, and M. Zhu, *J. Chromatogr.*, **346**, (1985) 265.

15. S. Terabe, K. Otsuka, and T. Ando, *Anal. Chem.*, **57**, (1985) 834.

16. B. A. Bidlingmeyer,*Practical HPLC Methodology and Applications*, John Wiley & Sons, New York, 1992.

17. C. F. Poole, and S. A. Schuette,*Contemporary Practice of Chromatography*, Elsevier, Amsterdam, 1984.

18. S. G. Perry, and P. O. Brewer,*Practical Liquid Chromatography*, Plenum Press, New York, 1972.

19. L. R. Snyder,*Principles of Adsorption Chromatography*, Plenum Press, New York, 1968.

20. T. Halicioglu, and O. Sinanoglu, *Ann. N. Y. Acad. Sci.*, **158**, (1969) 308.

21. C. Horvath, W. Melander, and I. Molnar, *Anal. Chem.*, **49**, (1977) 142.

22. F. P. B. v. d. Maeden, *J. Chromatogr.*, **149**, (1978) 539.

23. V. Ling, *Anal. Chem.*, **63**, (1991) 2909.

24. J. C. Harrison, in *Protein Phosphorylation - A Pratical Research* (Hardie, D. G., ed), Oxford University Press, New York, 1992, 22.

25. M. Dole, L. L. Mack, and P. L. Hines, *J. chem. Phys*, **49**(3), (1968) 2240-2249.

26. J. B. Fenn, M. Mann, C. K. Meng, S. F. Wong, and C. M. Whitehouse, *Science*, **246**, (1989) 64-71.

27. M. Yamashita, and J. B. Fenn, *J. Chem. Phys.*, **88**, (1984) 4451-4459.

28. M. Yamashita, and J. B. Fenn, *J. Chem. Phys.*, **88**, (1984) 4671-4675.

29. R. D. Smith, J. A. Loo, C. G. Edmons, C. J. Barinage, and H. R. Udseth, *Anal. Chem.*, **62**, (1990) 882.

30. M. Mann, *Org. Mass Spectrom.*, **25,** (1990) 575.

31. M. G. Ikonomou, A. T. Blades, and P. Kebarle, *Anal. Chem.*, **62,** (1990) 957.

32. P. Kebarle, and L. Tang, *Anal. Chem.*, **65,** (1993) 972A.

33. P. Thibault, C. Paris, and S. Pleasance, *J. Rapid Commun. Mass Spectrom.*, **5,** (1991) 484.

34. R. Feng, Y. Konishi, and A. W. Bell, *J. Am. Soc. Mass Spectrom.*, **2,** (1991) 387.

35. R. D. Smith, J. A. Loo, C. G. Edmonds, C. J. Barinaga, and H. R. Udseth, *Anal. Chem.*, **62,** (1990) 882.

36. V. Katta, and B. T. Chait, *J. Am. Chem. Soc.*, **113,** (1991) 8534.

37. M. Baca, and S. B. H. Kent, *J. Am. Chem. Soc.*, **114,** (1992) 3392.

38. K. J. Wahl, *J. Am. Chem. Soc.*, **115,** (1993) 803.

39. K. J. Wahl, B. L. Schwatz, and R. D. Smith, *J. Am. Chem. Soc.*, **116,** (1994) 5271.

40. H. K. Lim, Y. L. Hsieh, B. Ganem, and J. Henion, *J. Am. Soc. Mass Spectrom.*, **30,** (1995) 708.

41. Y. L. Hsieh, J. Cai, Y. T. Li, and J. D. Henion, *J. Am. Soc. Mass Spectrom.*, **6,** (1995) 85.

42. M. Karas, and F. Hillenkamp, *Anal. Chem.*, **60,** (1988) 2299.

43. F. Hillenkamp, M. Karas, R. C. Beavis, and B. T. Chait, *Anal. Chem.*, **63,** (1991) 1193A.

44. R. J. Cotter, *Anal. Chem.*, **64,** (1992) 1027A.

45. F. Hillenkamp, M. Karas, D. Holtkamp, and P. Klusener, *Int. J. Mass Spectrom. Ion Phys*, **69**, (1986) 265.

46. A. Vertes, and R. Gilbels, *Chem. Phys. Lett.*, **171**, (1990) 284.

47. R. E. Johnson, and B. U. R. Sundquist, *Rapid Commun. Mass spectrom.*, **5**, (1991) 574.

48. J. V. Iribarne, and B. A. Thomson, *J. Chem. Phys.*, **64**, (1976) 2287.

49. W. C. Wiley, and J. B. Mclaren, *Rev. Sci. Instrum.*, **26**, (1955) 1150.

50. H. Wollnik, *Mass Spectrom Rev.*, **12**, (1993) 89.

51. R. C. Beavis, and B.T.Chait, *Chem. Phys. Lett.*, **181**, (1991) 479.

52. J. Zhou, W. Ens, K. Standing, and A. Verentchikov, *Rapid Commun. Mass Spectrom.*, **6**, (1992) 617.

53. R. S. Brown, and J. J. Lennon, *Anal. Chem.*, **67**, (1995) 1998.

54. S. M. Colby, T. B. King, and J. P. Reilly, *Rapid Commun. Mass Spectrom.*, **8**, (1994) 865.

55. R. M. Whittal, and L. Li, *Anal. Chem.*, **67**, (1995) 1950.

56. J. G. Boyle, and C. M. Whitehouse, *Anal. Chem.*, **64**, (1992) 2084.

57. P. E. Miller, and M. B. Denton, *J. Chem. Education*, **63**, (1986) 617.

58. C. N. McEwen, and B. S. Larsen, *Electrospray Ionization on Quadrupole and Magnetic-Sector Mass Spectrometers in Electrospray Ionization Mass Spectrometry- Fundamentals, Instrumentation, and Applications* (Cole, R. B., Ed.), Wiley, New York, 1997.

59. J. A. Olivares, N. T. Nguyen, C. R. Yonker, and R. D. Smith, *Anal. Chem.*, **59**, (1987) 1230.

60. R. D. Smith, J. A. Olivares, N. T. Nguyen, and H. R. Udseth, *Anal. Chem.*, **60**, (1988) 436.

61. R. D. Smith, C. Barinaga, and H. R. Udseth, *Anal. Chem.*, **60**, (1988) 1948.

62. E. D. Lee, W. Miick, J. D. Henion, and T. R. Covey, *Biomedical and Environmental Mass Spectrom.*, **18**, (1989) 844.

63. S. Pleasance, P. Thibault, and J. Kelly, *J. Chromatogr.*, **591**, (1992) 325.

64. D. C. Cale, and R. D. Smith, *J. Rapid Commun. Mass Spectrom.*, **7**, (1993) 1017.

65. K. Tsuji, L. Baczynskyj, and G. E. Bronson, *Anal. Chem.*, **64**, (1992) 1864.

66. T. J. Thompson, F. Foret, P. Vouros, and B. L. Karger, *Anal. Chem.*, **65**, (1993) 900.

67. J. H. Wahl, D. R. Goodlett, H. R. Udseth, and R. D. Smith, *Anal. Chem.*, **64**, (1992) 3194.

68. D. R. Goodlett, J. H. Wahl, H. R. Udseth, and R. D. Smith, *J. Microcol. Sep.*, **5**, (1993) 57.

69. F. Foret, T. J. Thompson, P. Vouros, and B. L. Karger, *Anal. Chem.*, **66**, (1994) 4450.

70. J. H. Wahl, D. C. Gale, and R. D. Smith, *J. Chromatogr.*, **659**, (1994) 217.

71. E. Gelpi, *J. Chromatogr.*, **703**, (1995) 59.

72. W. M. A. Niessen, and A. P. Tinke, *J. Chromatogr.*, **703**, (1995) 37.

73. P. J. Arpino, *Mass Spectrom. Rev.*, **3**, (1989) 35.

74. A. L. Yergey, C. G. Edmonds, I. A. S. Lewis, and M. Vestal, , Plenum Press, New York, 1990, 31-86.

75. R. M. Caprioli,*Continuous-flow Fast Atom Bombardment Mass Spectrometry*, Wiley, New York, 1990.

76. R. C. Willoughby, and R. F. Browner, *Anal. Chem.*, **56**, (1984) 2626.

77. *101 The API Book, PE Sciex*, Thornhill, Ontario, 1989.

78. C. M. Whitehouse, R. N. Dreyer, M. Yamashita, and J. B. Fenn, *Anal. Chem.*, **57**, (1985) 675.

79. J. B. Fenn, M. Mann, C. K. Meng, S. F. Wong, and C. M. Whitehouse, *Mass Spectrom. Rev.*, **9**, (1990) 37.

80. A. P. Bruins, T. R. Covey, and J. D. Henion, *Anal. Chem.*, **59**, (1987) 2642.

81. *Electrospray Ionization Mass Spectrometry-Fundamentals, Instrumentation, and Applications* (Cole, R. B., Ed.), Wiley, New York, 1997.

82. T. Covey, B. Sushan, R. Bonner, W. Schroder, and F. Hucho, in *Methods in Protein Sequence Analysis* (Jornvall, H., Hoog, J. O., and Gustavsson, A. M., eds), Birkhauser Verlag, Basel, 1991, 249.

83. M. J. Huddleston, M. F. Bean, and S. A. Carr, *Anal. Chem.*, **65**, (1993) 877.

ACKNOWLEDGMENTS

I would like to give my heartfelt appreciation to the following people for their contribution of time, faith, passion, support, encouragement or friendship throughout the whole study.

My husband Zhouxin Shen, my parents Jinhe Wei and Zhizhen Shi, my grandmother Shumin Wu, my sister Wei Wei, and all of my aunts and uncle. To all of my former and present group members and my friends: Liyu Yang , Elise Luong, Pamela Jensen, Yun Jiang, Yan Cao, Jean Kelly, Jay Xiu and Meng Sun.

I gratefully thank to Dr. Cheng S. Lee for his guidance and encouragement throughout my graduate study.

I am very grateful to Dr. Donald J. Graves for his solid support and expert advises for my research especially in the last several months. His expert guidance, enthusiasm and encouragement made my third project exciting and enjoyable.

Drs. Dennis C. Johnson, Carole A. Heath, , and Patricia A. Thiel honored me by investing time and showing interest in my project. I would like to express my appreciation to them.

I thank Dr. Kamel A. Harrata for his collaboration and friendship.

Instrumentation Center of the Institute for Physical Research and Technology at Iowa

State University.

IMAGE EVALUATION
TEST TARGET (QA-3)

150mm

6″
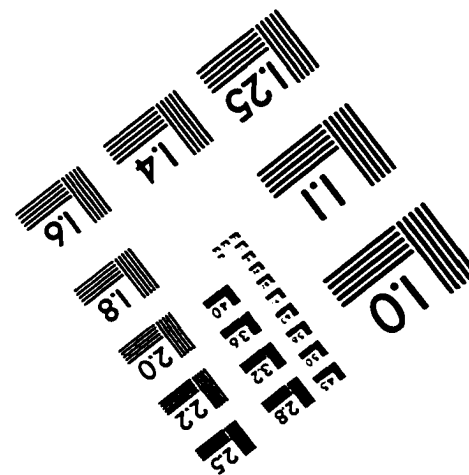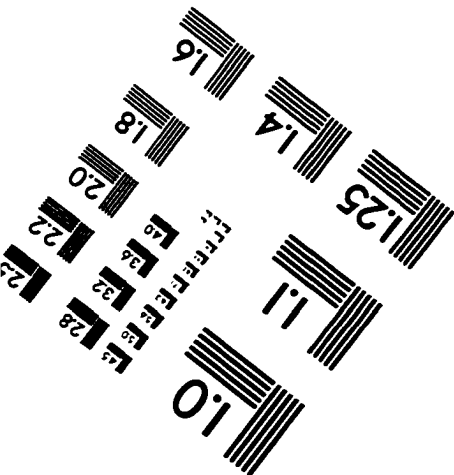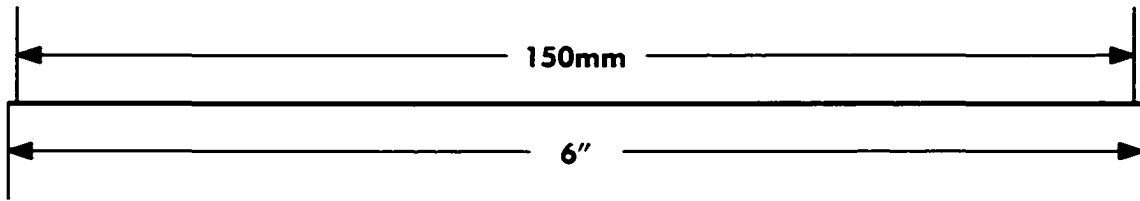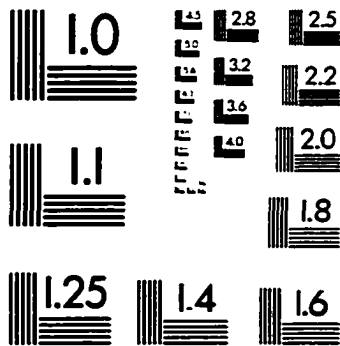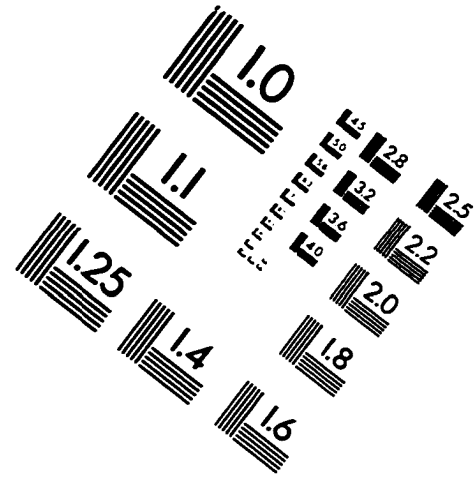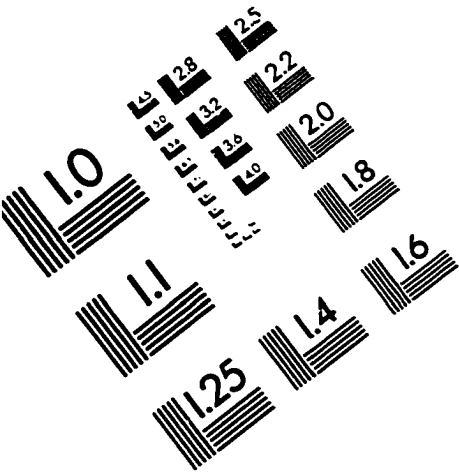
APPLIED IMAGE . Inc
1653 East Main Street
Rochester, NY 14609 USA
Phone: 716/482-0300
Fax: 716/288-5989